NASA TECHNICAL MEMORANDUM

NASA TM X-71965

COPY NO.

NASA TM X-71965

AN ANALYTICAL STUDY OF THE EFFECTS OF JETS LOCATED MORE THAN ONE JET DIAMETER ABOVE A WING AT SUBSONIC SPEEDS

By Lawrence E. Putnam

May 1974

This informal documentation medium is used to provide accelerated or special release of technical information to selected users. The contents may not meet NASA formal editing and publication standards, may be revised, or may be incorporated in another publication.

NATIONAL AERONAUTICS AND SPACE ADMINISTRATION
LANGLEY RESEARCH CENTER, HAMPTON, VIRGINIA 23665

1. Report No.	2. Government Accession No.	3. Recipient's Catalog No.
TM X-71965		

4. Title and Subtitle	5. Report Date
An Analytical Study of the Effects of Jets Located More Than One Jet Diameter Above A Wing at Subsonic Speeds	May 1974
	6. Performing Organization Code
7. Author(s)	8. Performing Organization Report No.
Lawrence E. Putnam	
	10. Work Unit No.
9. Performing Organization Name and Address	501-24-06-01
NASA Langley Research Center Hampton, VA 23665	11. Contract or Grant No.
	13. Type of Report and Period Covered
12. Sponsoring Agency Name and Address	Technical Memorandum
National Aeronautics and Space Administration Washington, DC 20546	14. Sponsoring Agency Code

15. Supplementary Notes

Interim Technical Information Release, subject to possible revision and/or later formal publication

16. Abstract

A procedure has been developed to calculate the effects of blowing two jets over a swept tapered wing at low subsonic speeds. The algorithm used is based on a vortex lattice representation of the wing lifting surface and a line sink-source distribution to simulate the effects of the jet exhaust on the wing lift and drag. The method is limited to those cases where the jet exhaust does not intersect or wash the wing. The predictions of this relatively simple procedure are in remarkably good agreement with experimentally measured interference lift and interference induced drag.

17. Key Words (Suggested by Author(s)) (STAR category underlined)	18. Distribution Statement
Aerodynamics Interference Lift — Upper-Surface Blowing Interference Drag — Swept Wings Jet Effects — Tapered Wings Subsonic Flow	Unclassified - Unlimited

19. Security Classif. (of this report)	20. Security Classif. (of this page)	21. No. of Pages	22. Price*
Unclassified	Unclassified	48	$3.25

*Available from { The National Technical Information Service, Springfield, Virginia 22151 / STIF/NASA Scientific and Technical Information Facility, P.O. Box 33, College Park, MD 20740

AN ANALYTICAL STUDY OF THE EFFECTS OF JETS LOCATED MORE THAN ONE JET DIAMETER ABOVE A WING AT SUBSONIC SPEEDS

By Lawrence E. Putnam
Langley Research Center

SUMMARY

A procedure has been developed to calculate the effects of blowing two jets over a swept tapered wing at low subsonic speeds. The algorithm used is based on a vortex lattice representation of the wing lifting surface and a line sink-source distribution to simulate the effects of the jet exhaust on the wing lift and drag. The method is limited to those cases where the jet exhaust does not intersect or wash the wing. The predictions of this relatively simple procedure are in remarkably good agreement with experimentally measured interference lift and interference induced drag.

The results of the analytical study have indicated that substantial increases in wing lift and reductions in wing induced drag can occur when jets are blown over a wing. The magnitude of these effects increase with increasing ratio of jet exit velocity to free-stream velocity. The results also indicate that the interference effects are the most favorable when the nozzle exits are located ahead of or at the wing leading edge and inboard near the wing center line. The present method does not correctly predict the effects of jet vertical location at heights less than approximately 1.5 jet exit diameters; however, as the jet vertical location is reduced to this height the favorable effects of blowing jets over a wing increase.

INTRODUCTION

Recently, there has been renewed interest in locating the propulsion systems of future jet transport airplanes forward and above the wing. This unconventional engine location can take two forms. In one form, the jet is exhausted tangential to the wing upper surface to take advantage of Coanda turning of the jet exhaust as it passes over the wing to achieve high lift (refs. 1 through 4). In the second form the jet exhaust is raised so that the exhaust flow does not attach to the wing to avoid the cruise drag penalties associated with the first form. In both cases the jet noise propagated downward during takeoff and landing may be reduced by the shielding effects of the wing (refs. 5 and 6). In addition to noise shielding benefits, locating the propulsion system forward may also alleviate mass balance problems associated with advanced supersonic transport airplane concepts and may improve the wing flutter characteristics of such airplanes. To date, however, except for references 7 through 9, there is very little information available for use in assessing the effects of over wing jet blowing on subsonic or supersonic cruise performance and on climb performance of future jet transport airplanes.

The purpose of the present study was, therefore, to investigate analytically the effects of blowing jets over wings on subsonic cruise and climb performance. An elementary analytical procedure based on the vortex lattice theory for the wing and the theory of reference 10 for a jet exhausting into a subsonic stream has been developed to calculate the effects of blowing one or two jets over a swept tapered wing. As a result of the basic assumptions, the method is limited to the second case where the jet exhaust does not intersect or wash the wing. As long as the jet is sufficiently high such that it does not violate the above condition the effects of jet to free-stream velocity ratio (i.e. jet thrust coefficient), location of the jet exhaust relative to the wing, nozzle exit diameter, wing leading edge sweep, wing aspect ratio, and wing taper ratio on the lift and drag induced by blowing jets over a wing at subsonic speeds can be analytically investigated.

SYMBOLS

Ae	exit area per nozzle
AR	wing aspect ratio, $\frac{b^2}{S_{ref}}$
b	wing span
C_A	axial force coefficient
$C_{D,i}$	induced drag coefficient
$\Delta C_{D,i}$	$(C_{D,i})$ jet on - $(C_{D,i})$ jet off
C_{D_o}	drag coefficient at zero lift
C_L	lift coefficient
ΔC_L	(C_L) jet on - (C_L) jet off
C_N	normal force coefficient

c	wing chord or chord of elemental vortex lattice panel
c_l	section lift coefficient
d_e	nozzle exit diameter
K_I	slope of line source or line sink distribution
l_c	length of chordwise vortex-line segment on wing
l_{core}	length of core of jet exhaust plume
M_e	Mach number of jet at nozzle exit
M_∞	free stream Mach number
N	number of points or number of elemental vortex lattice panels
$p_{t,e}$	total pressure of jet at nozzle exit
p_∞	free stream static pressure
Q	strength of line source or sink distribution

q_e	dynamic pressure of jet at nozzle exit
q_∞	free stream dynamic pressure
S_{ref}	reference area (wing planform area)
s	semi-width of horseshoe vortex
U_e	velocity of jet at nozzle exit
U_∞	free stream velocity
u_i, v_i, w_i	circulation induced perturbation-velocity components in positive X-, Y-, and Z- directions
$u_{jet}, v_{jet}, w_{jet}$	jet induced perturbation-velocity components in positive X-, Y-, and Z- directions
V_e	effective velocity ratio $\sqrt{\frac{\rho_\infty U_\infty^2}{\rho_e U_e^2}}$
V_r	radial velocity in jet axis system induced by line sink-source distribution

X, Y, Z	orthogonal right-handed primary Cartesian coordinate system with origin at wing apex (see figure 1). Positive X-direction is forward, positive Y-direction is toward right wing tip, and positive Z-direction is downward. X-Y plane parallel to wing chord plane
X_J, R_J	jet cylinderical coordinate system with origin at nozzle exit (figure 3); positive X-direction is in direction of jet exhaust
x, r	cylinderical coordinates associated with jet
$x_{c/4}$	longitudinal location in primary Cartesian coordinate system of midspan of quarter-chord of elemental panel
$x_{3c/4}$	longitudinal location in primary Cartesian coordinate system of midspan of three-quarter-chord of elemental panel
x_e, y_e, z_e	primary Cartesian coordinates of nozzle exit
x_{l_e}	primary Cartesian X-coordinate of wing leading edge at y_e
y_{cp}	primary Cartesian Y-coordinate of control point on elemental panel

α	angle of attack, deg
Γ	circulation strength
γ_e	ratio of specific heats of jet at nozzle exit
γ_∞	ratio of specific heats of free stream
ζ	dummy variable of integration
η	fraction of wing semispan from wing root chord in Y-direction
η_e	location of jet axis in fraction of wing semispan, $\frac{2y_e}{b}$
θ	camber angle of wing at control point, deg
Λ	sweep angle, deg
$\Lambda_{c/4}$	wing quarter chord sweep angle, deg
Λ_{le}	wing leading edge sweep angle

λ	taper ratio, $\frac{c_t}{c_r}$
ρ_e	density of jet at nozzle exit
ρ_∞	free stream density

Subscripts

av	average
c	chordwise
r	root
s	spanwise
t	tip
total	total

METHOD OF ANALYSIS

The algorithm used in the present study to calculate the effects of blowing exhaust jets over a swept tapered wing is based on a vortex lattice representation of the wing lifting surface and a line source-sink distribution to represent the effects of the exhaust jets. The method, which has been programmed for a digital computer, assumes that the flow external to the jet exhaust is steady, irrotational, inviscid, and incompressible. It

was also assumed that the jet is not deflected by the free stream, the jets does not intersect or wash the wing, and the jet cross sectional shape is not distorted by the wing flow field or by any crossflow components of the free stream velocity. A typical wing planform and engine arrangement for which the effects of blowing jets over the wing can be calculated with the present method is shown on figure 1.

The vortex lattice method used to represent the wing lifting surface is based on references 11 and 12. Each half of the wing is subdivided in both the spanwise and chordwise directions into 50 or less elemental areas. In the present computer program the number of spanwise and number of chordwise panels is arbitrary; however, unless otherwise specified, all calculations for the present study were made with 5 equal spaced chordwise and 10 equal spaced spanwise divisions on each half of the wing. Each elemental area is represented by a horseshoe vortex with the bound portion lying along the local quarter-chord-line of the element. (See figure 2.) The trailing vortices lie streamwise along the inboard and outboard edges of each panel on the wing chord plane. Aft of the wing trailing edge, the trailing vortices continue in the chordwise direction, that is, it is assumed that the trailing vortices are not turned by the wing downwash or by the free stream velocity. Note that this is not the conventional method of locating the trailing vortices parallel to the free stream velocity as used in reference 12, but is similar to the formulation of reference 11. The boundary condition that the flow be tangential to the wing surface is satisfied for each element at a point on the lateral mid-point of the local three-quarter-chord line of the element.

The induced effects of the jet exhaust were simulated with a distribution of line sinks and sources located on the longitudinal axis of the jet. The axis of the jet was divided into a number of segments over which the sink or source strength was assumed to be linear. This continuous line sink-source distribution is equivalent

to a series of triangular elemental distributions as illustrated in figure 3. The radial velocity induced by the jet at a point in the surrounding flow field is therefore given by the following equation:

$$V_r(x,r) = \frac{K_1 r}{4\pi} \int_{x_1}^{x_2} \frac{(x_2 - \zeta)\, d\zeta}{\left[(x-\zeta)^2 + r^2\right]^{3/2}}$$

$$+ \sum_{I=2}^{N-1} \frac{K_I r}{4\pi} \left\{ \frac{(x_I - x_{I-1})}{(x_{I+1} - x_I)} \int_{x_I}^{x_{I+1}} \frac{(x_{I+1} - \zeta)d\zeta}{\left[(x-\zeta)^2 + r^2\right]^{3/2}} \right.$$

$$\left. + \int_{x_{I-1}}^{x_I} \frac{(\zeta - x_{I-1})d\zeta}{\left[(x-\zeta)^2 + r^2\right]^{3/2}} \right\} + \frac{K_N r}{4\pi} \int_{x_{N-1}}^{x_N} \frac{(\zeta - x_N)d\zeta}{\left[(x-\zeta)^2 + r^2\right]^{3/2}}$$

The strength of each elemental line source or sink was adjusted to give the inflow velocity on the boundary of the jet predicted by the method of reference 10. In the present analysis only those interference effects resulting from the jet radial perturbation velocities are considered: any perturbation velocities induced parallel to the jet axis are neglected. In effect, therefore, the interference effects of the jet on the wing are attributed to an upwash distribution along the wing lifting surface.

To determine the circulation strength of each elemental horseshoe vortex on the wing, the following equation for the circulation induced downwash velocity must be satisfied at each control point on the wing:

$$\frac{w_i}{U_\infty} = \frac{\sin(\alpha + \Theta)}{\cos \Theta} - \frac{w_{jet}}{U_\infty} - \frac{u_{jet}}{U_\infty} \tan \Theta$$

A sketch illustrating this boundary condition at each control point is shown on figure 4. It is apparent from this sketch how the induced effects of the jet modify the boundary condition equation. Note that in the present formulation the u_{jet} perturbation velocity only arises when the axis of the jet is not parallel to the wing chord plane.

After the circulation strengths for the horseshoe vortices are determined, the forces acting on the wing can be determined. From reference 11, the forces acting on each spanwise segment of vortex filament in coefficient form are:

$$C_{A,s} = \frac{2\Gamma_s}{U_\infty} \left| \frac{w_i}{U_\infty} + \frac{w_{jet}}{U_\infty} - \sin \alpha \right| \left[\frac{2s}{S_{ref}} \right]$$

$$C_{N,s} = \frac{2\Gamma_s}{U_\infty} \left| \left(\frac{v_i}{U_\infty} + \frac{v_{jet}}{U_\infty} \right) \tan \Lambda - \frac{u_i}{U_\infty} - \frac{u_{jet}}{U_\infty} + \cos \alpha \right| \left[\frac{2s}{S_{ref}} \right]$$

For each chordwise segment of vortex filament the force coefficients are:

$$C_{A,c} = 0$$

$$C_{N,c} = \frac{2\Gamma_c}{U_\infty} \left[\frac{v_i}{U_\infty} + \frac{v_{jet}}{U_\infty} \right] \frac{l_c}{S_{ref}}$$

Where Γ_c is the net circulation strength resulting from the individual circulations of each trailing horseshoe vortex leg forming that segment. The total normal force and axial force acting on the wing are obtained by summing the normal and axial forces acting on all segments. The lift and induced drag coefficients are then obtained from:

$$C_L = C_{N,total} \cos \alpha - C_{A,total} \sin \alpha$$

$$C_{D,i} = C_{A,total} \cos \alpha + C_{N,total} \sin \alpha$$

This solution for the induced drag is equivalent to the near field solution of reference 12. The integration of the wing span load distribution (the far field method) to obtain the induced drag is not applicable to the present problem. Because of the induced upwash field generated by the jet exhaust the assumption inherent in the far field method are violated. (See refs. 13 and 14.)

DISCUSSION

Comparison of Present Method with Other Theoretical Methods and with Experiment

To verify the vortex lattice algorithm used to represent the wing in the present method, the computed lift and drag characteristics of an aspect ratio 8 straight wing without a jet have been compared to the predictions of reference 12. (See fig. 5.) The present computer

algorithm gives essentially the same results as reference 12 for each of the cases considered: a flat wing, a wing with Clark Y camber distribution, and a twisted wing with no camber. There are some small discrepancies in the results of the two methods at the higher angles of attack. This small discrepancy is associated with the nonlinearization of the boundary conditions in the present method. Note that the near field induced drag results of reference 12 are compared with the present method.

Experimental investigations of the effects of blowing jets over a wing are very scarce; in particular for the case where the jet is sufficiently high such that it does not wash the wing. One source of such data is reference 15. The comparison of the present method with these experimental results shown on figure 6 indicates very good agreement at vertical locations of the jet exhaust greater than 1.5 nozzle exit diameters above the wing. In general, the effects of jet to free-stream velocity ratio, longitudinal location of the jet, and vertical distance of the jet above the wing on the interference lift are well predicted. As the jet approaches the wing, however, the experimental results show a significant increase in interference lift over the predicted values. This discrepancy results when the jet washes the wing and Coanda turning of the jet with its associated increase in interference lift occurs. This effect of Coanda turning of the jet exhaust is of course neglected in the present method.

A comparison of the present method with the experimental data of reference 9 for two jets blowing over a 50° swept leading edge wing with an aspect ratio of 3 and a taper ratio of 0.3 is shown on figure 7. These experimental data were obtained at nozzle exit total pressure to free-stream static pressure ratios from approximately 1 to 6 and at free-stream Mach numbers of 0.4, 0.6, and 0.7. The theory of reference 10 was derived for an incompressible jet exhausting into an incompressible external stream with no density difference between the two streams. The

variable density case can be related to the incompressible constant density solution of reference 10 with an effective velocity ratio (ref. 16) as defined in the following equation

$$V_e = \sqrt{\frac{\rho_\infty U_\infty^2}{\rho_e U_e^2}} = \sqrt{\frac{q_\infty}{q_e}} = \frac{M_\infty}{M_e} \sqrt{\frac{\gamma_\infty p_\infty}{\gamma_e p_{t,e}}} \left[1 + \frac{(\gamma_e - 1)}{2} M_e^2\right]^{\frac{\gamma_e}{2(\gamma_e - 1)}}$$

For an air jet with $\gamma_e = \gamma_\infty = 1.4$

$$V_e = \frac{M_\infty}{M_e} \frac{\left[1 + 0.2 M_e^2\right]^{7/4}}{\sqrt{p_{t,e}/p_\infty}}$$

As shown on figure 7 (a) and 7 (b) the effective velocity ratio satisfactorily correlates the interference lift and the interference induced drag resulting from blowing two jets over the 50° swept leading edge wing of reference 9 at Mach numbers from 0.4 to 0.7. The predictions of the present method are in good agreement with the experimental results. These results indicate that the present method can be extended to the case where the jet and free stream are compressible and at different densities by use of the effective velocity ratio concept. An illustration of the application of the present method using the effective velocity ratio concept to the prediction of the effects on lift and induced drag due to blowing jets over a wing is shown on figure 7 (c) for the 50° swept wing of reference 9. The following equations were used to obtain the predicted lift and induced drag when the jets were blowing over the wing:

$$C_{L,\text{predicted}} = (C_{L,\text{jet off}})_{\text{measured}} + \Delta C_{L,\text{predicted}} \quad \text{at a given } \alpha$$

$$(C_{D,i})_{\text{predicted}} = ((C_{D,i})_{\text{jet off}})_{\text{measured}} + (\Delta C_{D,i})_{\text{predicted}} \quad \text{at a given } C_L$$

The predicted lift and drag characteristics using the present method to calculate the effects of the jets with the above equations are in good agreement with the experimental results. Of particular interest is the experimentally indicated improvement in induced drag (not necessarily in total drag) due to blowing two jets over the wing and the similar predictions of the present method.

Effect of Vortex Lattice Arrangement

Shown on figure 8 is the effect of the number of elemental chordwise panels on the predicted lift and induced drag of an aspect ratio 8, taper ratio 0.3 wing having the quarter chord swept 0^o with and without two jets blowing over the wing. It is apparent that there is essentially no effect of varying the number of elemental panels on the predicted lift and induced drag of the wing or on the increments in lift and drag due to jet blowing. Varying the number of spanwise elemental panels does result in a change in the predicted lift and induced drag for the wing with and without jet blowing. (See fig. 9.) It appears, however, that the interference effect due to jet blowing is not a strong function of the number of elemental vortex lattice panels. Therefore, regardless of the vortex lattice arrangement used, the predicted effects of jet blowing are essentially uneffected. Therefore 5 chordwise and 10 spanwise elemental panels have been used for all calculations of the present paper.

Effect of Velocity Ratio

The predicted effects of effective velocity ratio on the interference lift and interference induced drag due to jet blowing are shown on figures 6, 7, and 10 for an aspect ratio 2 straight wing, an aspect ratio 3, taper ratio 0.3 wing with 50° swept leading edge, and an aspect ratio 8, taper ratio 0.3 wing with 30° swept quarter chord, respectively. The present method predicts an increase in interference lift coefficient with increasing jet blowing (that is, increasing $1/V_e$). This favorable interference effect is essentially uneffected by angle of attack. The present method also predicts a decrease in induced drag with increasing ratio of jet velocity to free-stream velocity $1/V_e$. This favorable increment in interference induced drag increases with lift coefficient. On figure 10 (b) are shown typical calculations of the effects of effective velocity ratio on wing span load distribution and on section lift coefficient. Increased jet blowing results in an increased distortion of the span load distribution. Note that this increased distortion does not imply increased induced drag since integration of the span load distribution to obtain induced drag is only valid for planar wings without external interference effects. As would be expected the span load does increase in the vicinity of the jet. Increasing jet blowing also increases the section lift coefficient over the entire wing span.

Effect of Jet Location

The predicted effects of jet location on the interference lift and interference induced drag due to two jets blowing over various wing configurations are shown on figures 6 and 11 through 14. Increasing the vertical distance of the jets above the wing (figs. 6 and 11) causes a decrease in the interference lift and a reduction in the favorable interference induced drag. Moving the nozzle exit ahead of the wing leading edge causes a small increase in

interference lift and a small increase in the favorable induced drag increment. (See fig. 12.) Moving the nozzle exit aft of the wing leading edge causes a decrease in the interference lift and a substantial reduction in the favorable induced drag increment. The calculations shown on figures 13 and 14 indicate that the closer the jets are located to the wing center line the more favorable the interference effects due to blowing two jets over a wing. This is indeed a fortuitous result since reference 4 indicates that for a two engine configuration the engine should be located inboard to minimize the engine-out effect on rolling moment associated with upper surface blowing configurations during takeoff and landing.

CONCLUDING REMARKS

A procedure has been developed to calculate the effects of blowing two jets over a swept tapered wing at low subsonic speeds. The algorithm used is based on a vortex lattice representation of the wing lifting surface and a line sink-source distribution to simulate the effects of the jet exhaust on the wing lift and drag. The method is limited to those cases where the jet exhaust does not intersect or wash the wing. The predictions of this relatively simple procedure are in remarkably good agreement with experimentally measured interference lift and interference induced drag.

The results of the analytical study have indicated that substantial increases in wing lift and reductions in wing induced drag can occur when jets are blown over a wing. The magnitude of these effects increase with increasing ratio of jet exit velocity to free-stream velocity. The results also indicate that the interference effects are the most favorable when the nozzle exits are located ahead of or at the wing leading edge and inboard near the wing ceter line. The present method does not

correctly predict the effects of jet vertical location at heights less than approximately 1.5 jet exit diameters; however, as the jet vertical location is reduced to this height the favorable effects of blowing jets over a wing increase.

REFERENCES

1. Riebe, John M.; and Davenport, Edwin E.: Exploratory Wind-Tunnel Investigation to Determine the Life Effects of Blowing Over Flaps from Nacelles Mounted Above the Wing. NACA Tech. Note 4298, June 1958.

2. Turner, Thomas R.; Davenport, Edwin E.; and Riebe, John M.: Low-Speed Investigation of Blowing From Nacelles Mounted Inboard and on the Upper Surface of an Aspect-Ratio - 7.0 35° Swept Wing with Fuselage and Various Tail Arrangements. NASA Memo 5-1-59L, June 1959.

3. Phelps, Arthur E., III: Aerodynamics of the Upper Surface Blown Flap. STOL Technology, NASA SP-320, Oct. 1972 pp 97-110.

4. Phelps, Arthur E., III; and Smith, Charles C., Jr.: Wind-Tunnel Investigation of an Upper Surface Blow Jet-Flat Powered-Lift Configuration. NASA TN D-7399, 1973.

5. Anon: Aircraft Engine Noise Reduction. NASA SP-311, 1972.

6. Dorsch, Robert G.; and Reshotko, Meyer: EBF Noise Tests with Engine Under-the-Wing and Over-the-Wing Configurations. STOL Technology, NASA SP-320, Oct. 1972, pp 455-473.

7. Kettle, D. J.; Kurn, A. G.; and Bagley, J. A. : Exploratory Tests on A Forward-Mounted Overwing Engine Installation. C. P. No. 1207, Brit. A.R.C., 1972.

8. Wimpress, John K.: Upper Surface Blowing Technology As Applied To the YC-14 Airplane. SAE Paper 730916, Oct. 1973.

9. Putnam, Lawrence E.: Exploratory Investigation at Mach Numbers From 0.40 to 0.95 of the Effects of Jets Blown Over a Wing. NASA TN D-7367, 1973.

10. Squire, H. B.; and Trouncer, J.: Round Jet In A General Stream. Report Aero. 1904, R.A.E., Jan. 1944.

11. Fox, Charles H., Jr.: Prediction of Lift and Drag for Slender Sharp-Edge Delta Wings in Ground Proximity. NASA TN D-4891, 1969.

12. Margason, Richard J.; and Lamar, John E.: Vortex-Lattice Fortran Program for Estimating Subsonic Aerodynamic Characteristics of Complex Planforms. NASA TN D-6142, 1971.

13. Pope, Alan: Basic Wing and Airfoil Theory, First Ed., McGraw-Hill Book Co., Inc., 1951, pp 200-203.

14. Cone, Clarence D., Jr.: The Theory of Induced Lift and Minimum Induced Drag of Nonplanar Lifting Systems. NASA TR R-139, 1962.

15. Falk, H.: The Influence of the Jet of a Propulsion Unit on Nearby Wings. NACA TM 1104, 1946.

16. Carter, Arthur, W.: Effects of Jet-Exhaust Location on the Longitudinal Aerodynamic Characteristics of a Jet V/STOL Model. NASA TN D-5333, 1969.

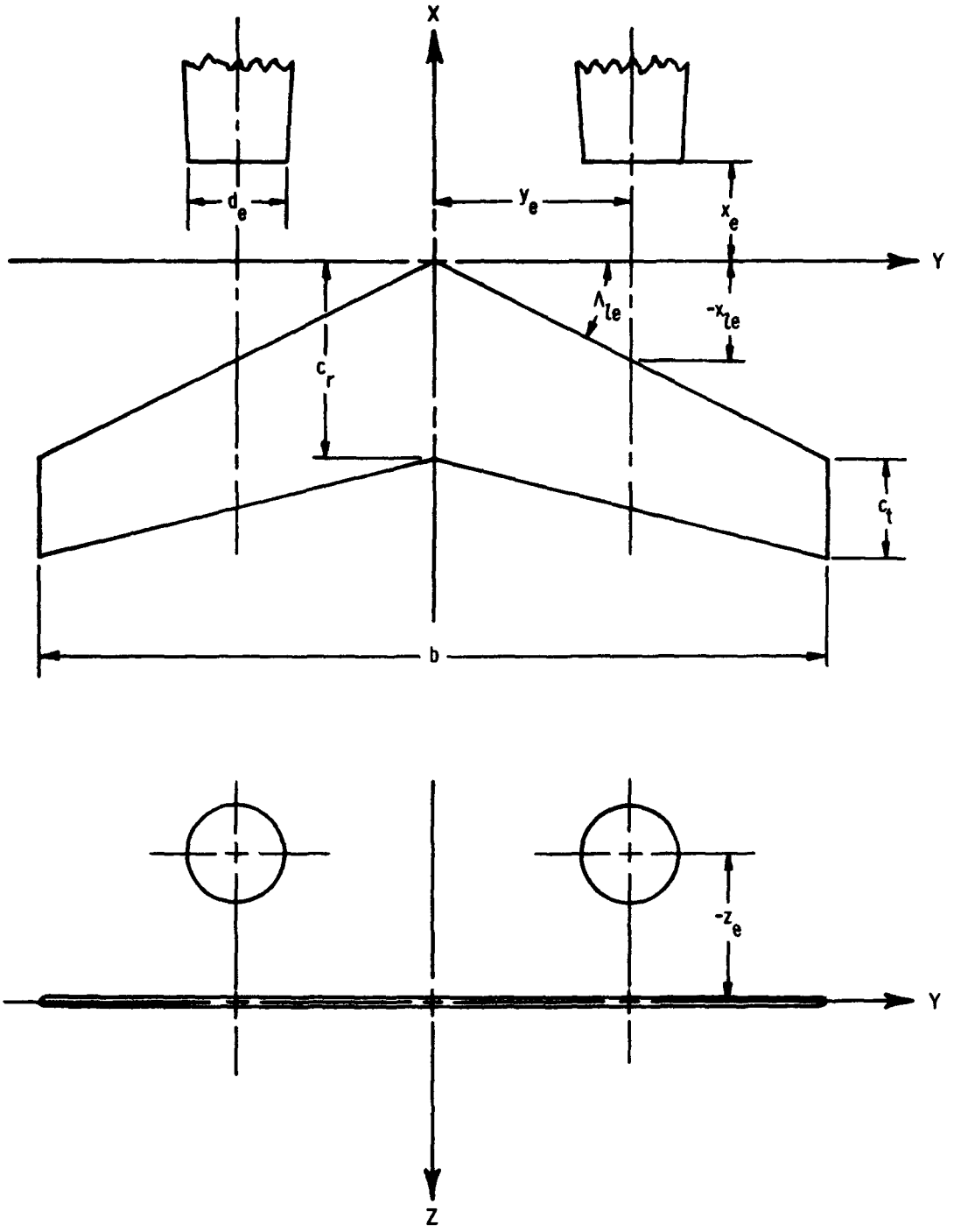

Figure 1.- General layout of a typical wing planform showing axis system and location of nozzle exits.

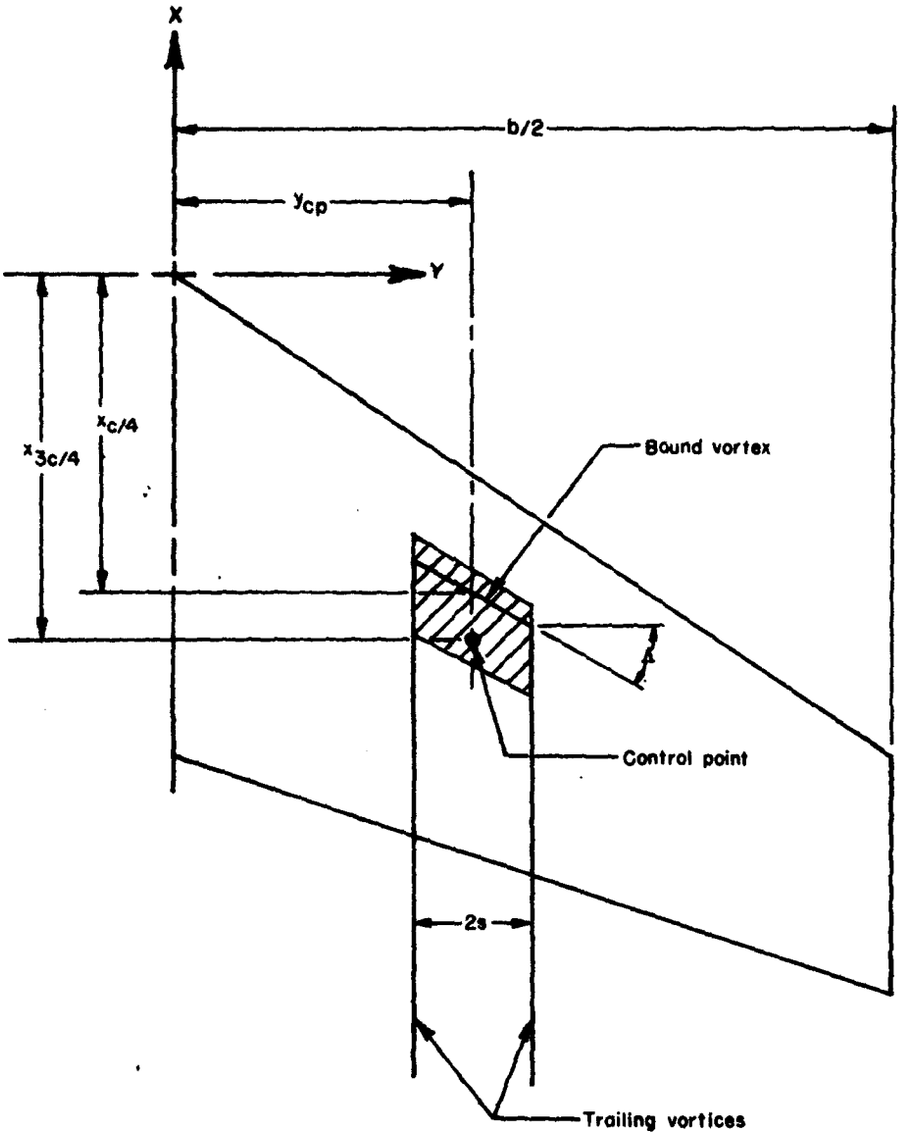

Figure 2.- Sketch of a typical elemental vortex-lattice panel on wing.

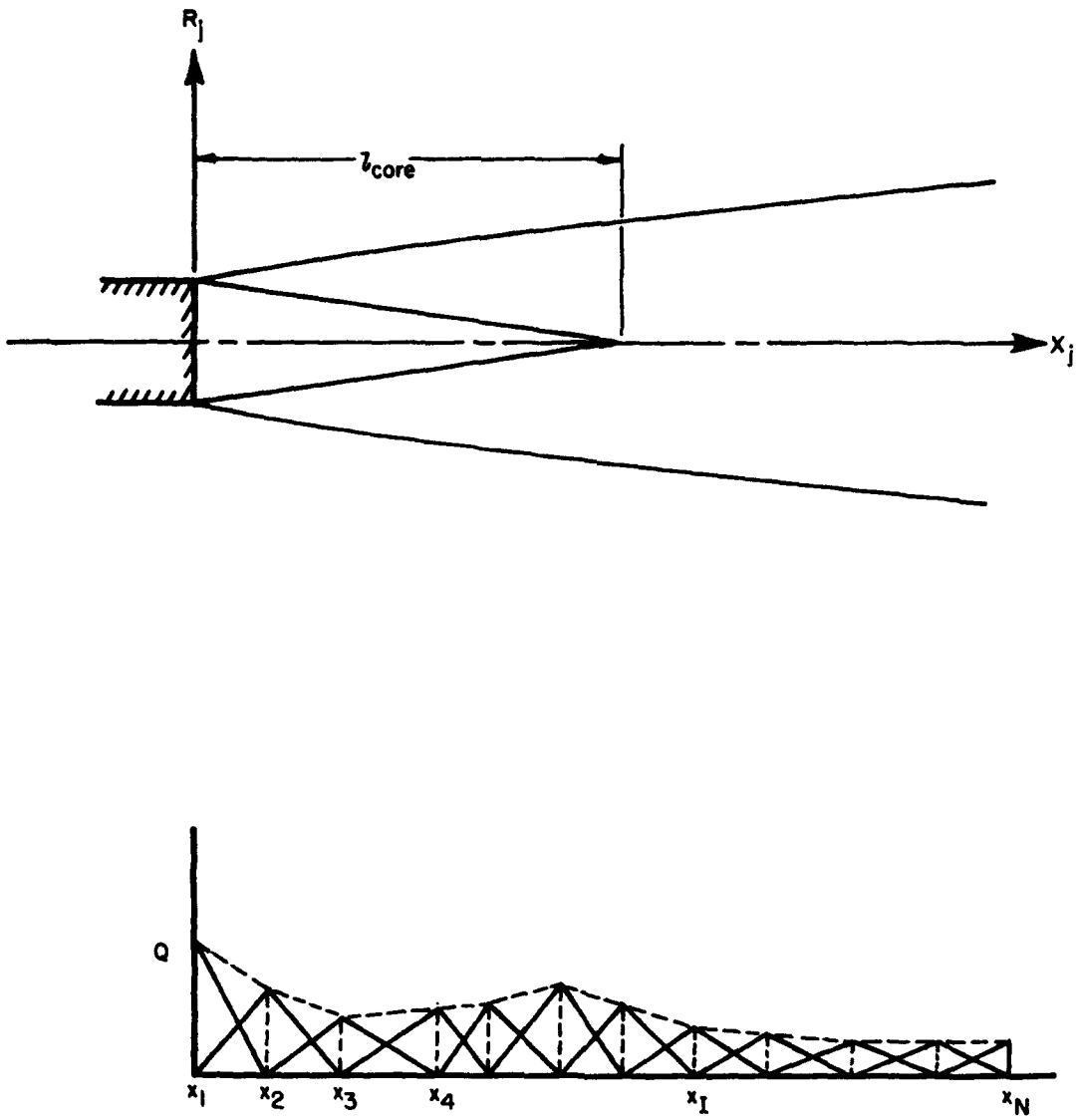

Figure 3.- Illustration of source-sink distribution used to represent effects of jet exhaust.

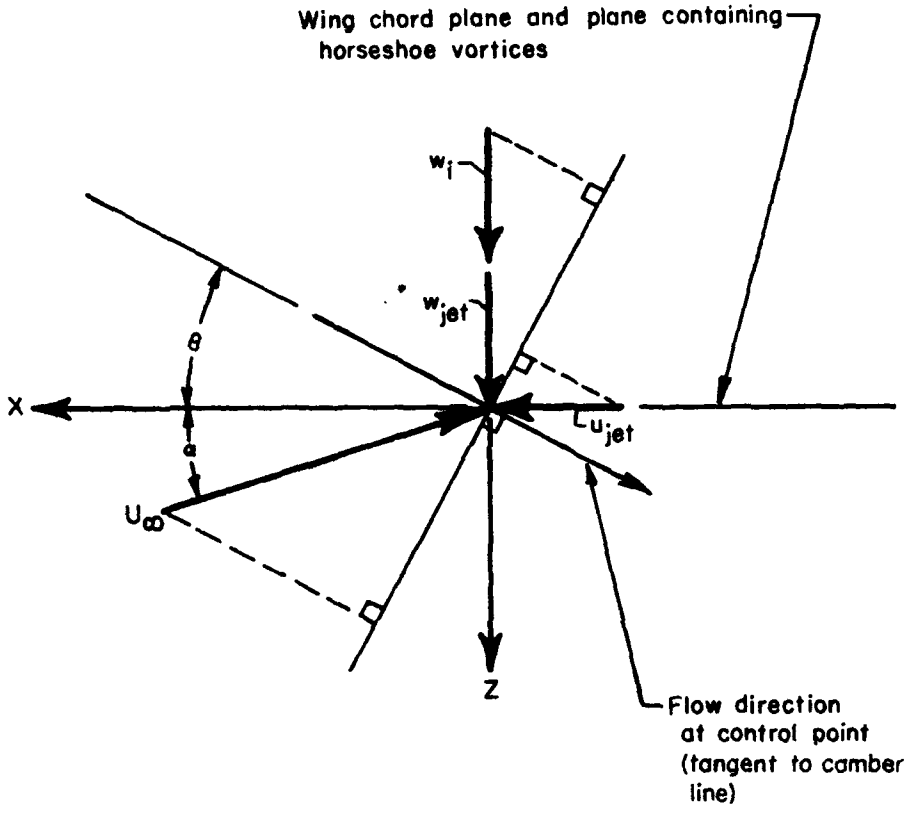

Boundary condition:

$$U_\infty \sin(\alpha + \theta) = (w_i + w_{jet}) \cos\theta + u_{jet} \sin\theta$$

Figure 4.- Sketch illustrating boundary conditions at each control point on wing.

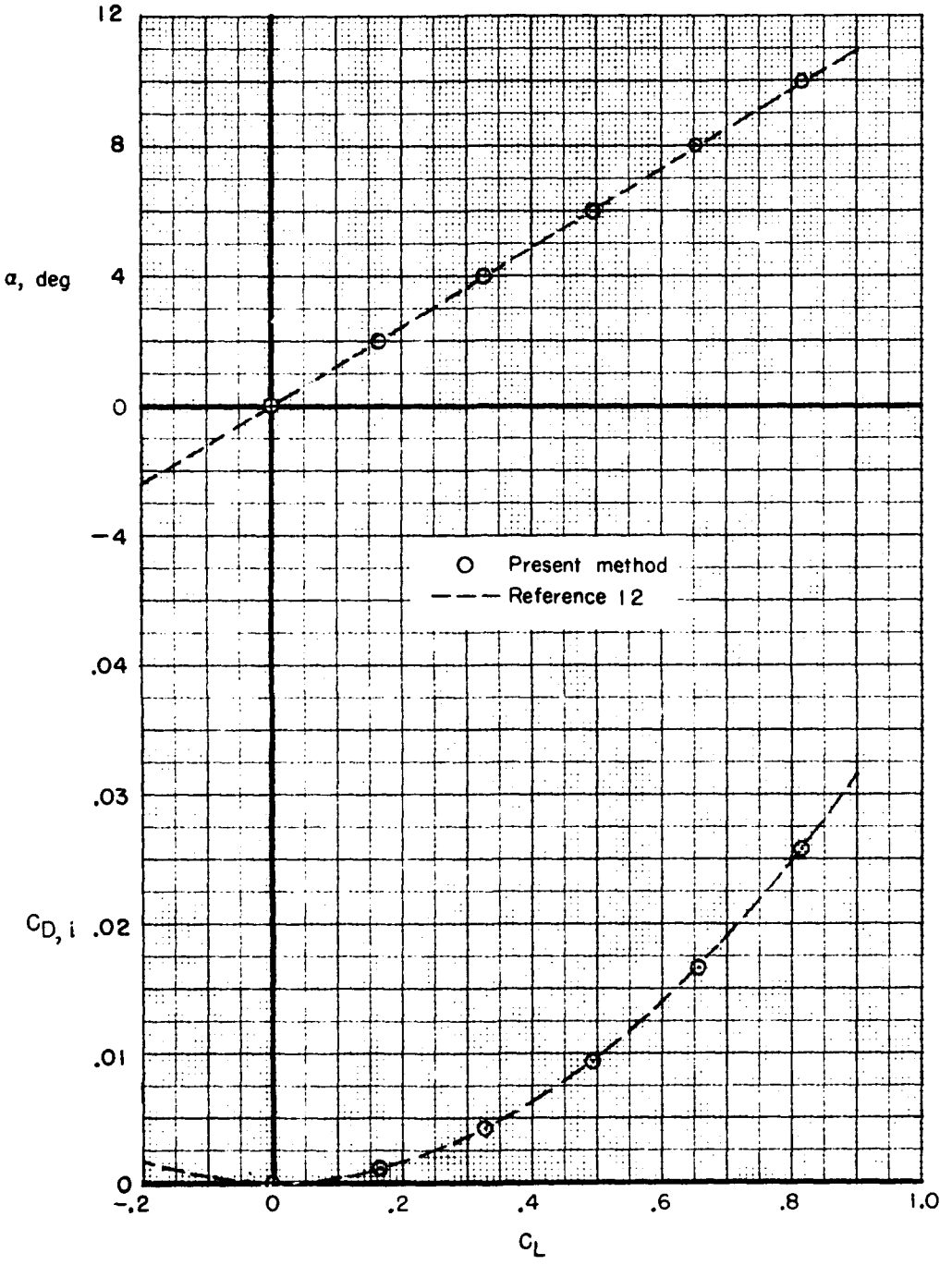

(a) Flat wing.

Figure 5.- Comparison of present method with that of reference 12 for an AR = 8, λ = 1.0 straight wing (jet off). (Reference 12 near field solution for induced drag shown.)

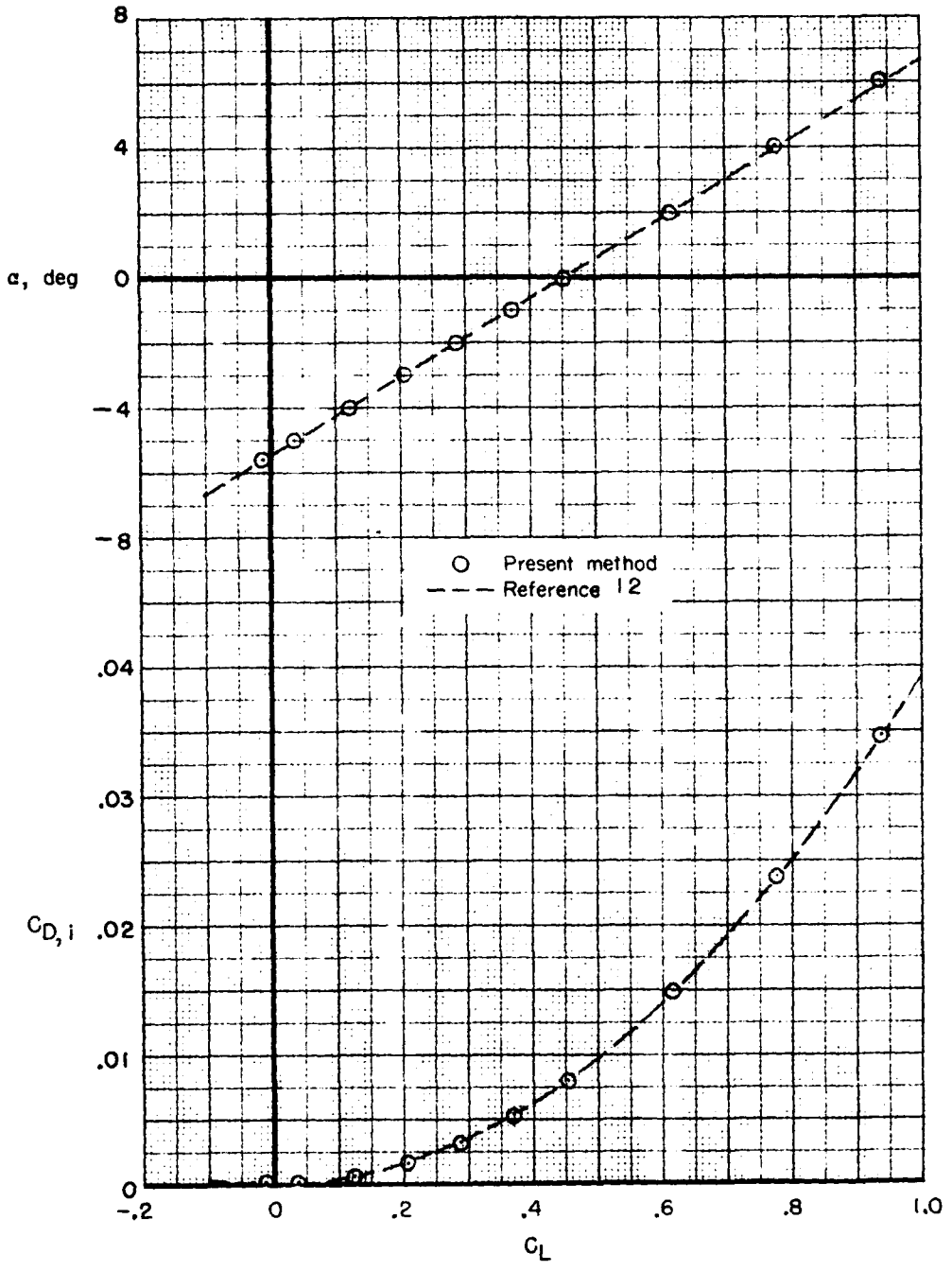

(b) Wing with Clark Y camber distribution.

Figure 5.- Continued.

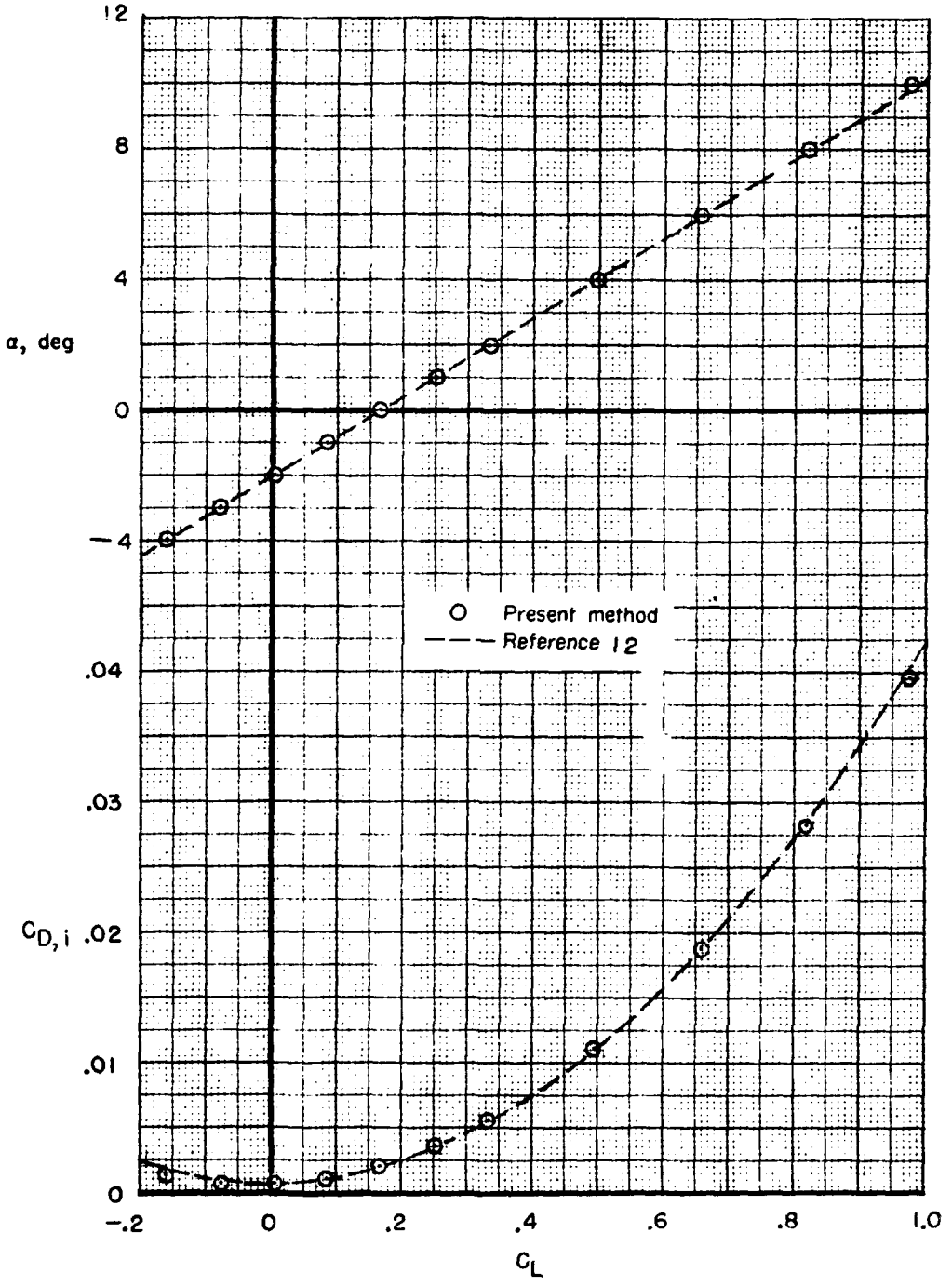

(c) Wing with twist distribution.

Figure 5.- Concluded.

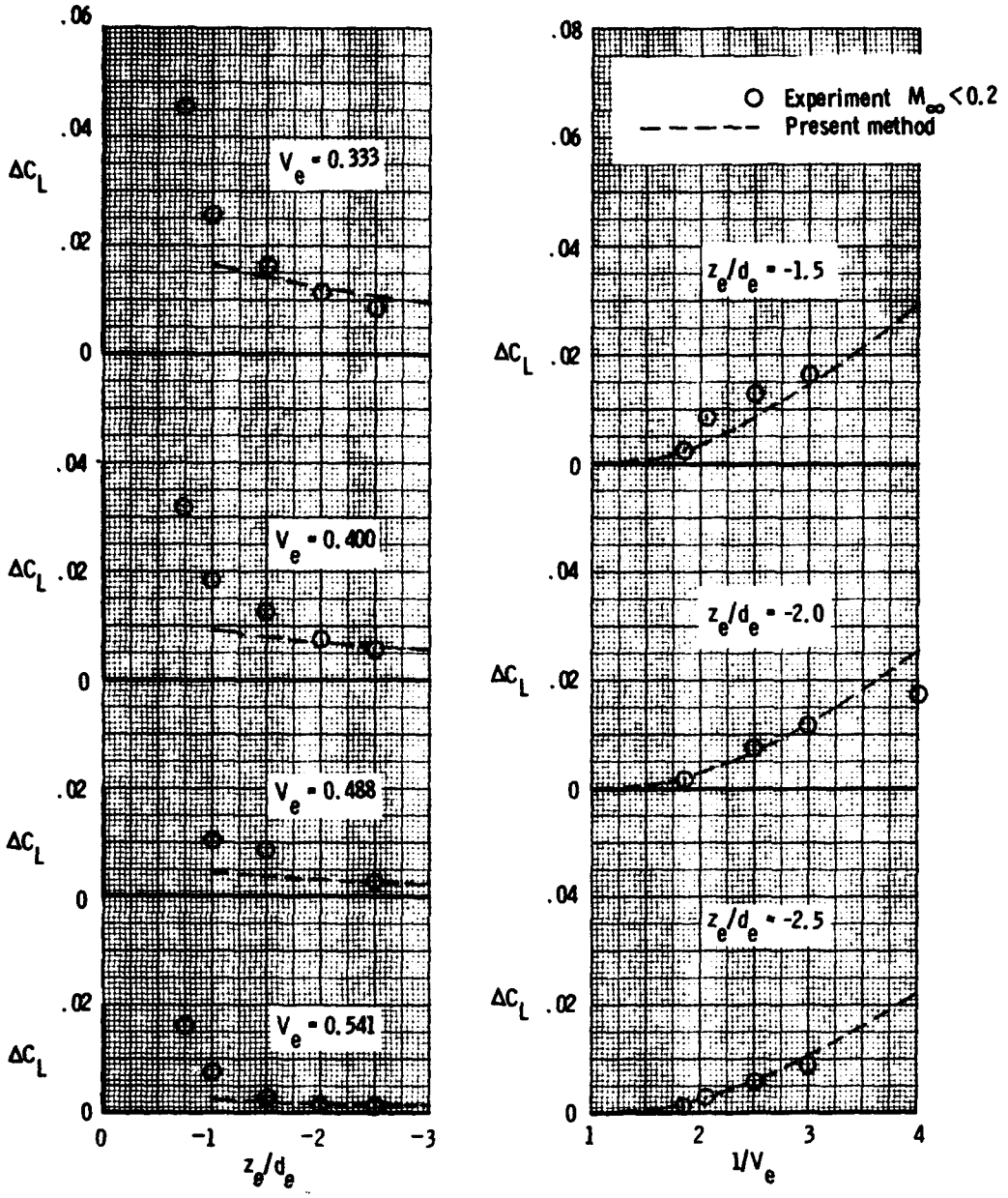

Figure 6. - Comparision of present method with experimental data of reference 15 for blowing one jet over an AR = 2, $\lambda = 1$ straight wing. $A_e/S_{ref} = 0.192$, $(x_e - x_{le})/d_e = 1.0$, $\eta_e = 0.0$, and $\alpha = 0°$.

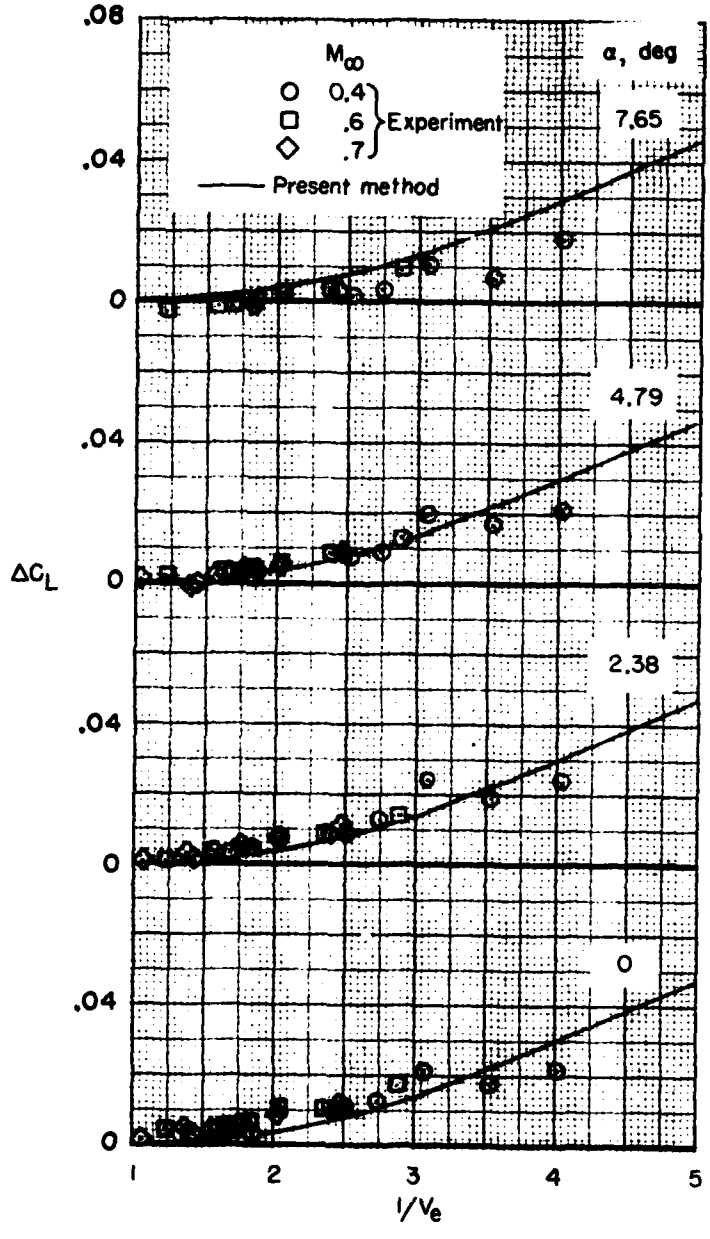

(a) Interference lift coefficient.

Figure 7.- Comparison of present method with experimental data of reference 9 for two jets blowing over a wing with AR = 3, $\lambda = 0.3$, and $\Lambda_{\ell e} = 50°$. $A_e/S_{ref} = 0.0078$, $(x_e - x_{\ell e})/d_e = 2.59$, $\eta_e = 0.46$, $z_e/d_e = -1.5$.

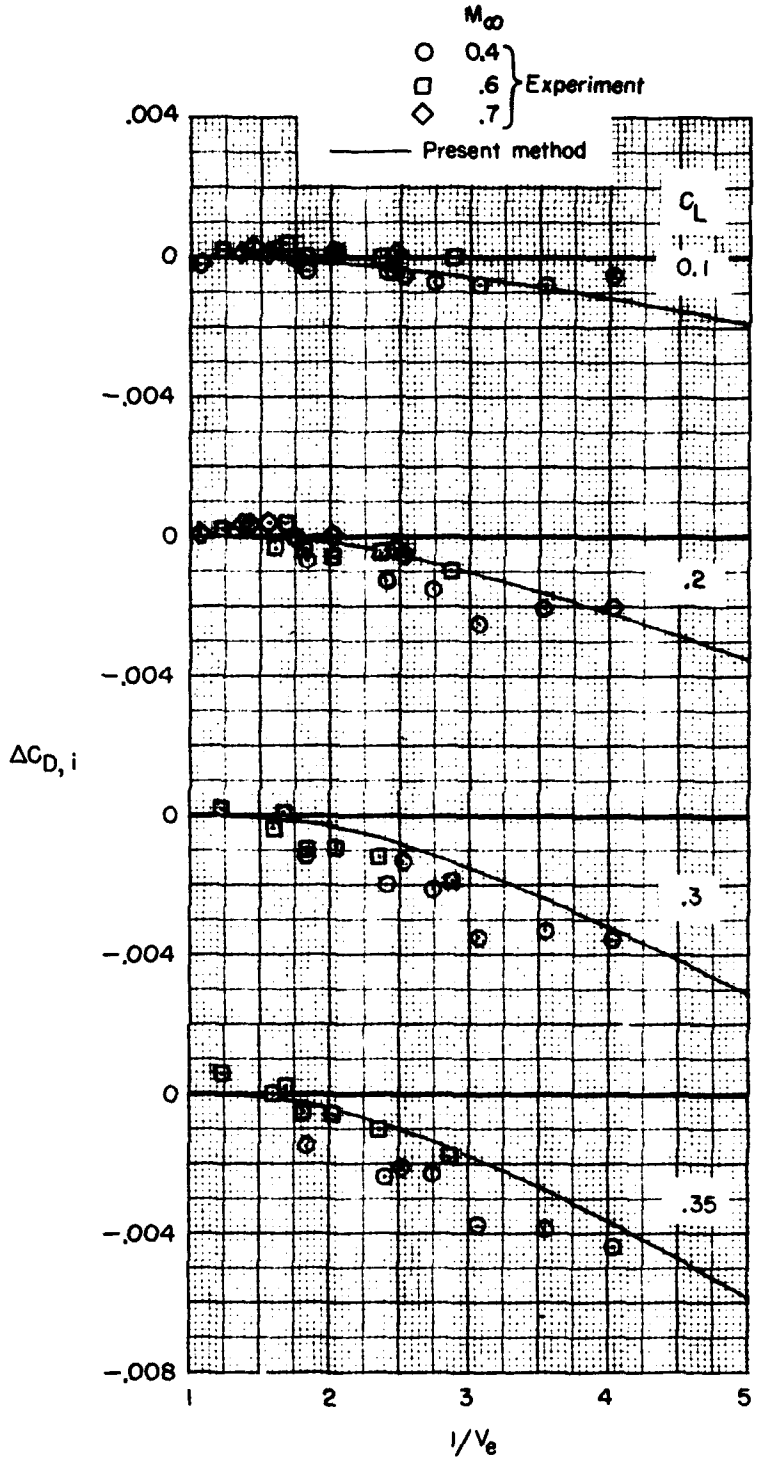

(b) Interference induced drag coefficient.

Figure 7.- Continued.

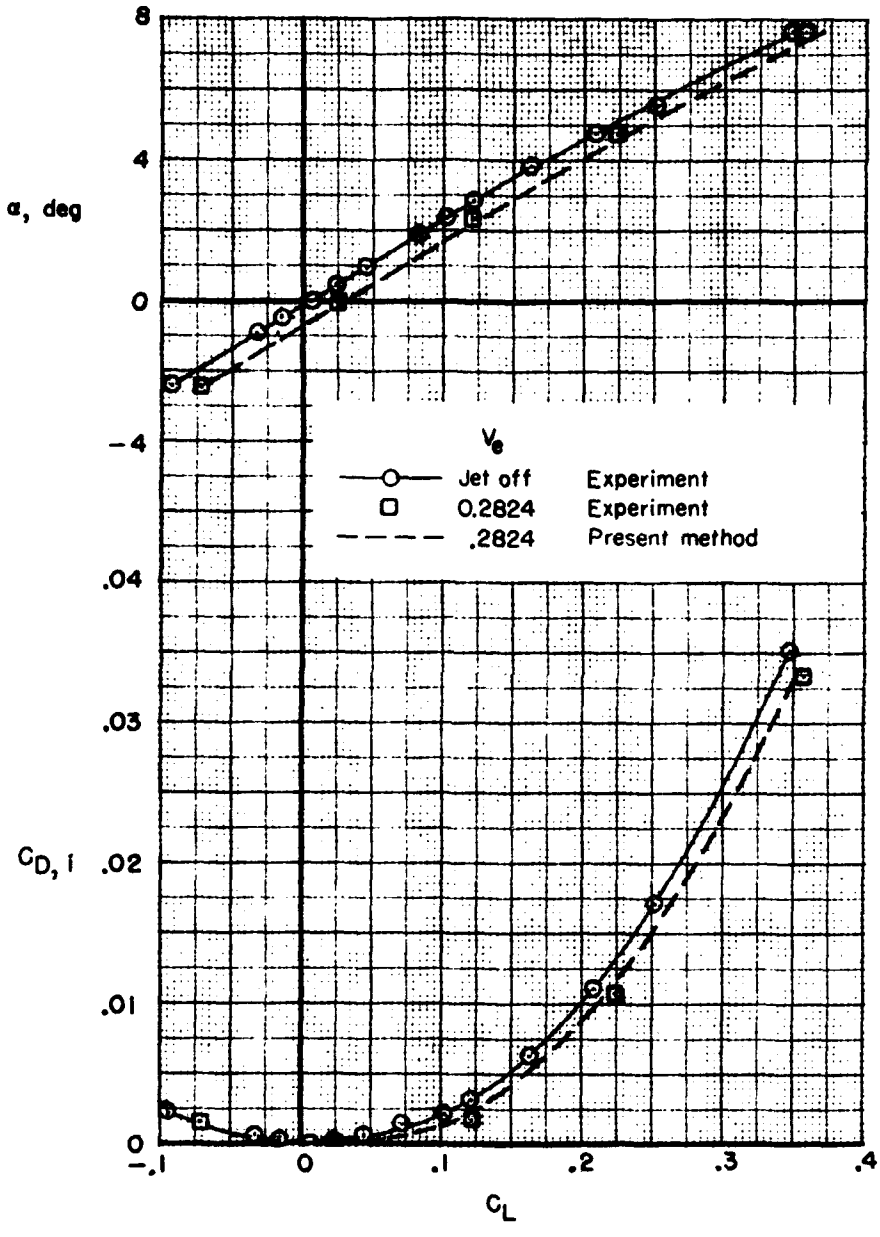

(c) Effect of jet blowing on lift and drag coefficient at $M_\infty = 0.40$.

Figure 7.- Concluded.

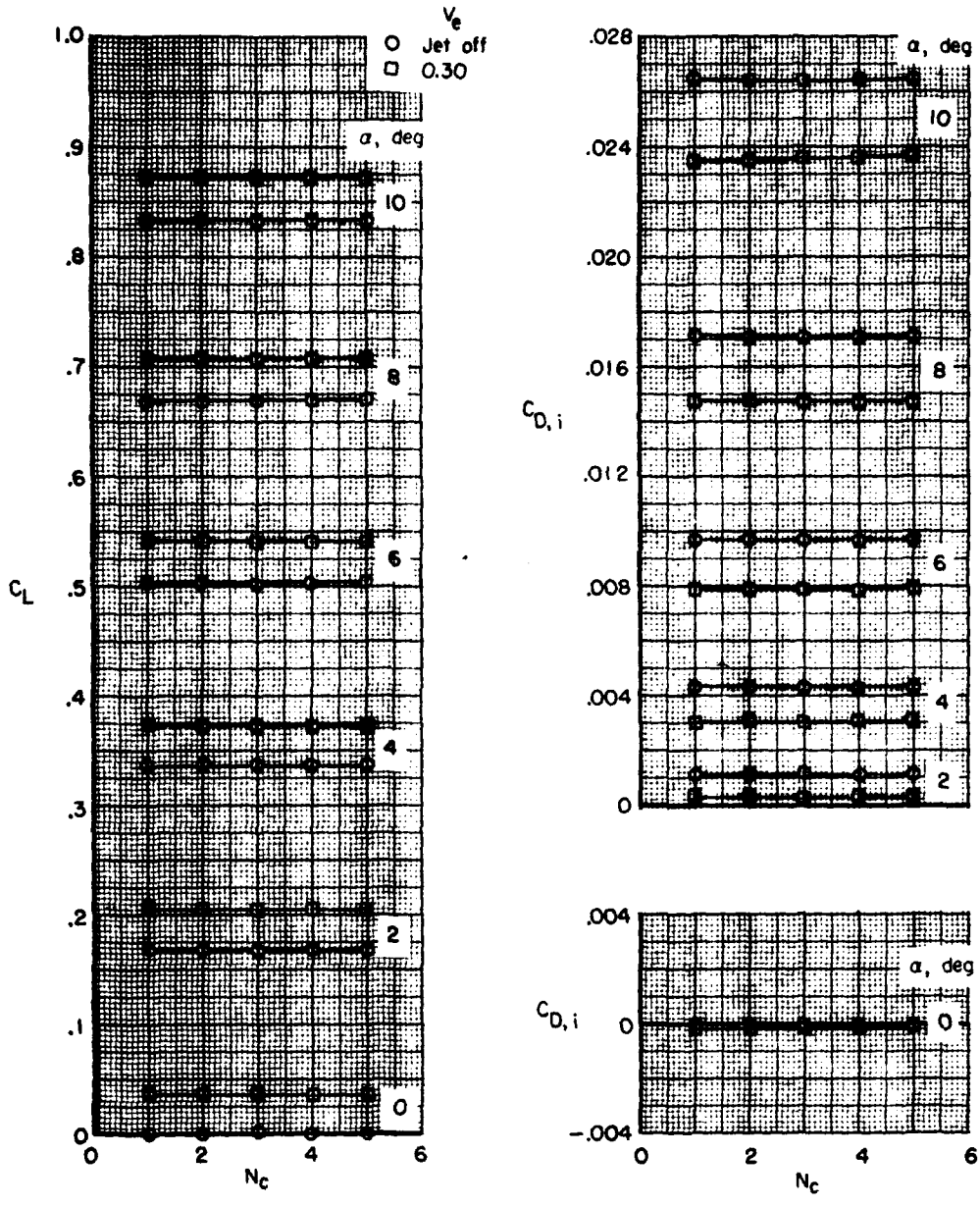

Figure 8.- Effect of number of chordwise elemental vortex lattice panels when N_s = 10 on the calculated lift and induced drag of a wing with AR = 8, λ = 0.3, and $\Lambda_{c/4}$ = 0° and with two jets having A_e/S_{ref} = 0.025 located at $(x_e - x_{le})/d_e$ = 0.0, η_e = 0.3, and z_e/d_e = -1.5.

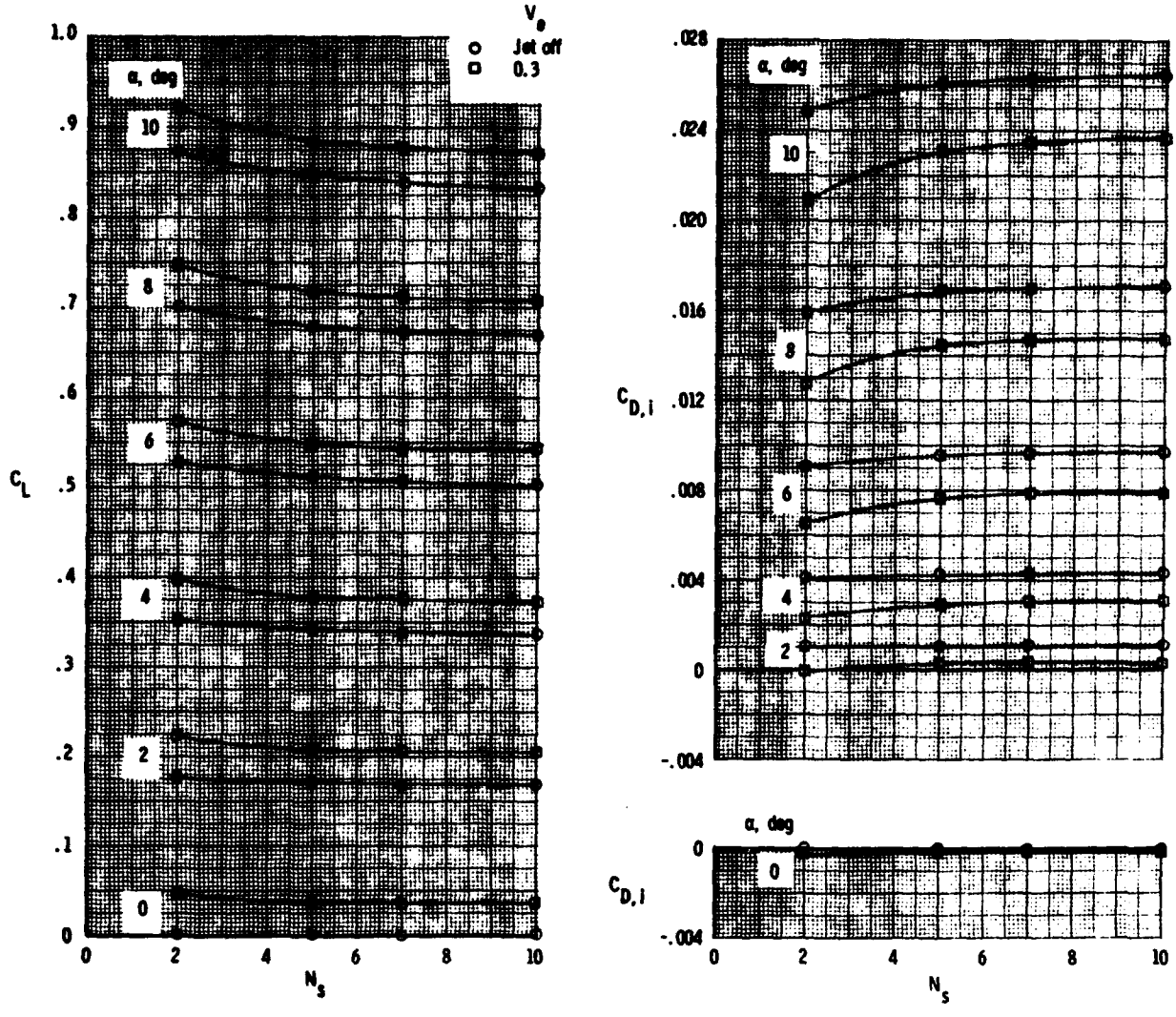

Figure 9. - Effect of number of spanwise elemental vortex lattice panels when $N_c = 5$ on the calculated lift and and induced drag of a wing with AR = 8, $\lambda = 0.3$, and $\Lambda_{c/4} = 0°$ and with two jets having $A_e/S_{ref} = 0.025$ located at $(x_e - x_{LE})/d_e = 0.0$, $\eta_e = 0.3$, and $z_e/d_e = -1.5$.

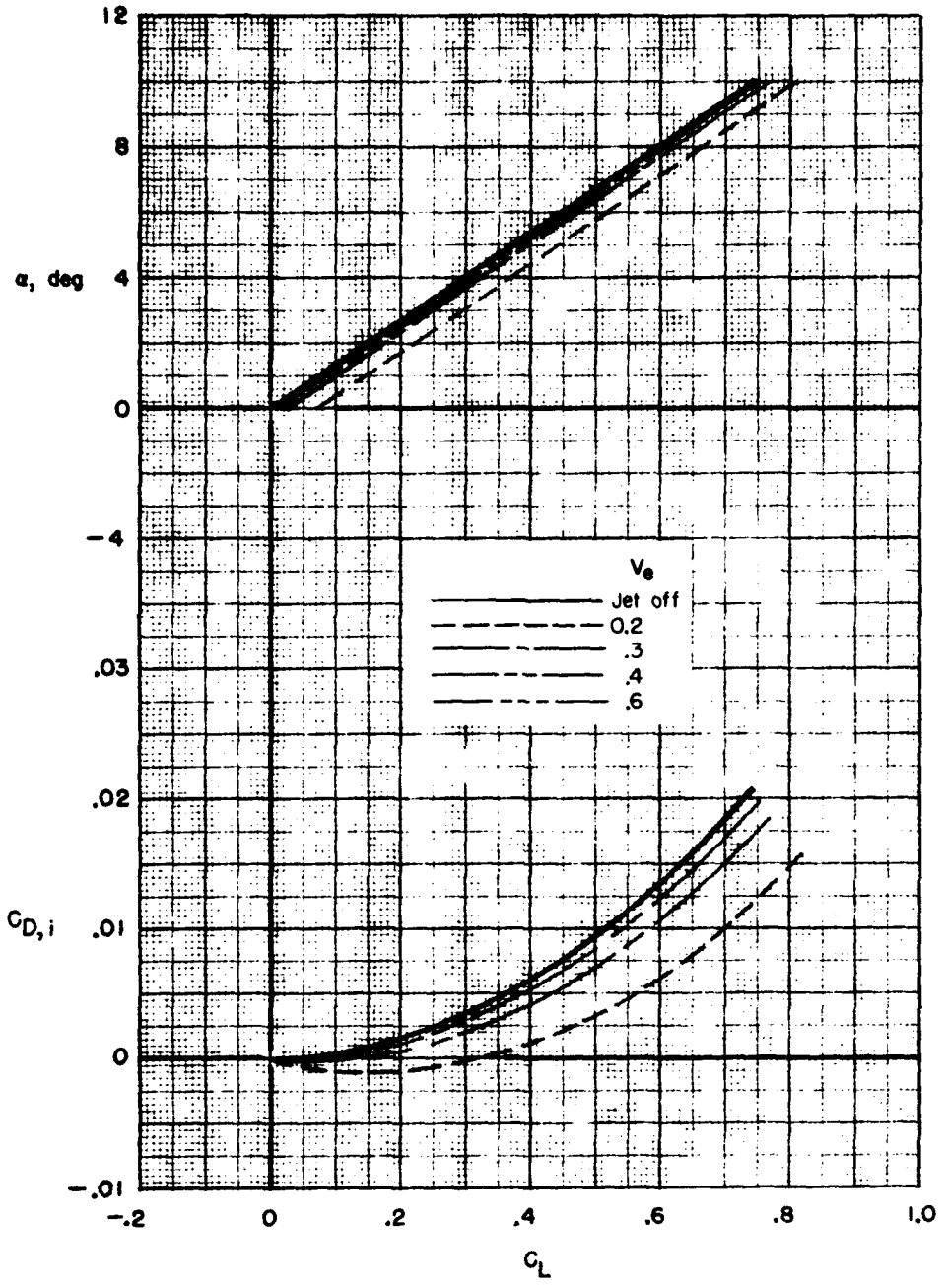

(a) Effect on C_L and $C_{D,i}$.

Figure 10.- Calculated effect of effective velocity ratio of two jets on aerodynamic characteristics of a wing with AR = 8, λ = 0.3, and $\Lambda_{c/4} = 30°$, $A_e/S_{ref} = 0.0125$, $(x_e - x_{le})/d_e = 0.0$, $\eta_e = 0.25$, $z_e/d_e = -1.401$.

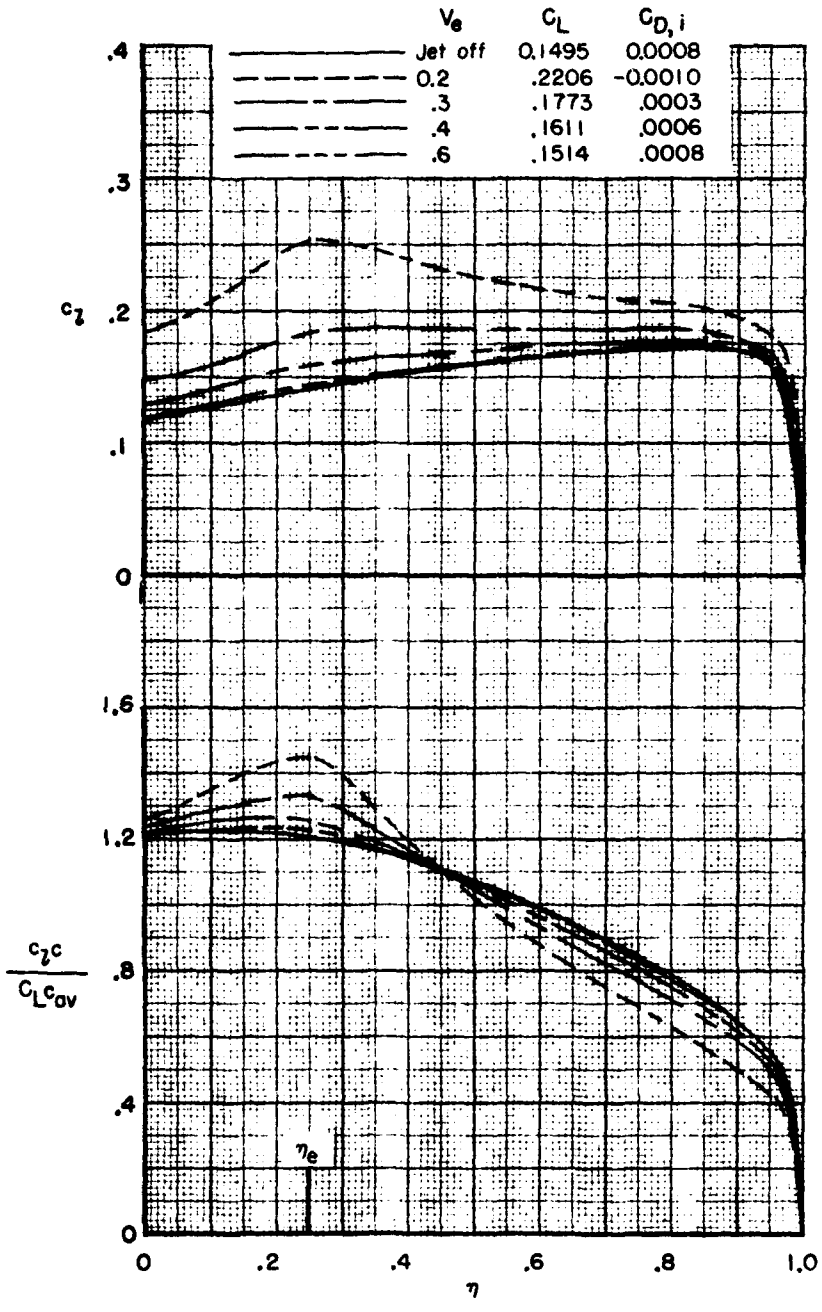

(b) Effect on span load distribution and section lift coefficient at $\alpha = 2^{\circ}$.

Figure 10.- Continued.

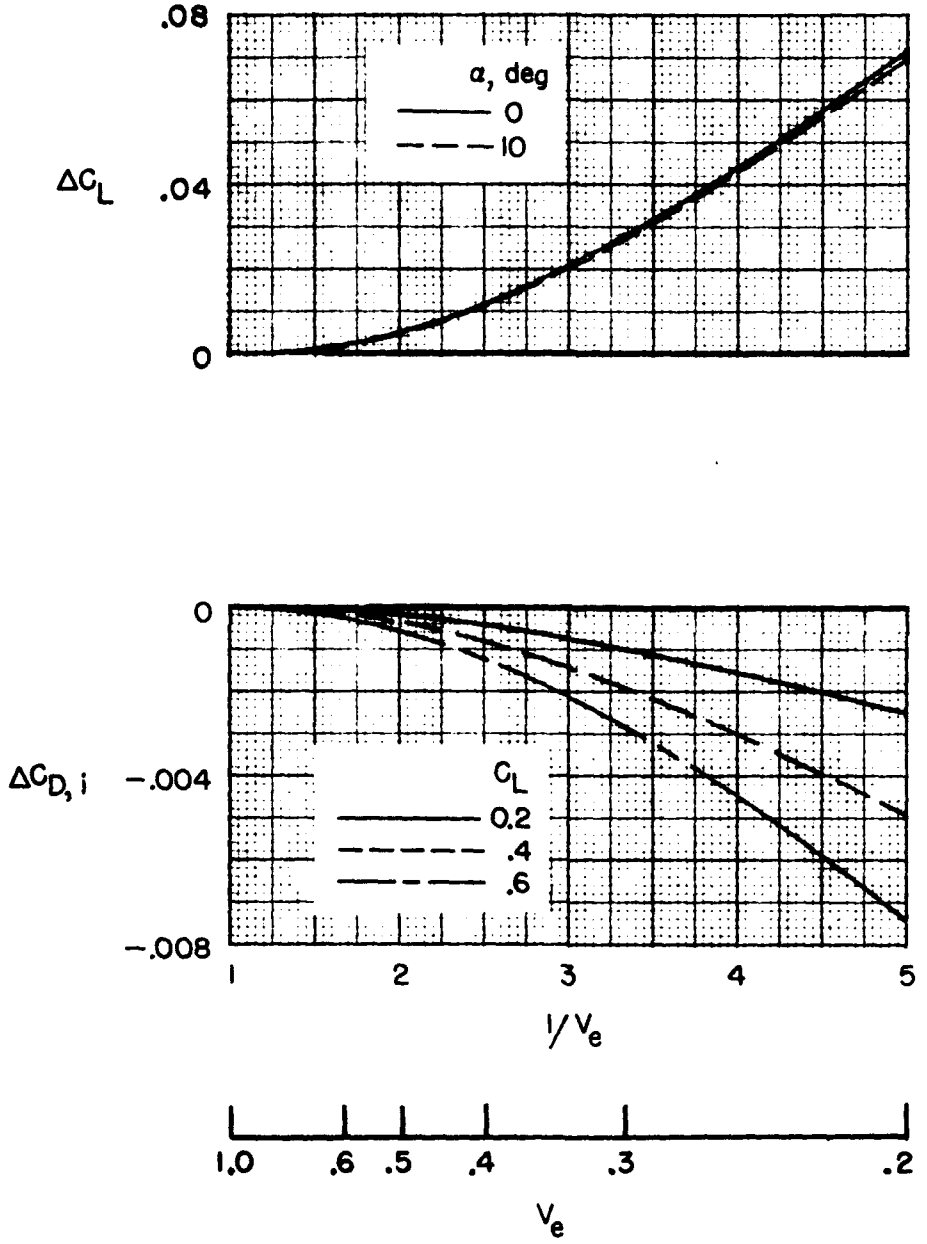

(c) Effect on ΔC_L and $\Delta C_{D,i}$.

Figure 10.- Concluded.

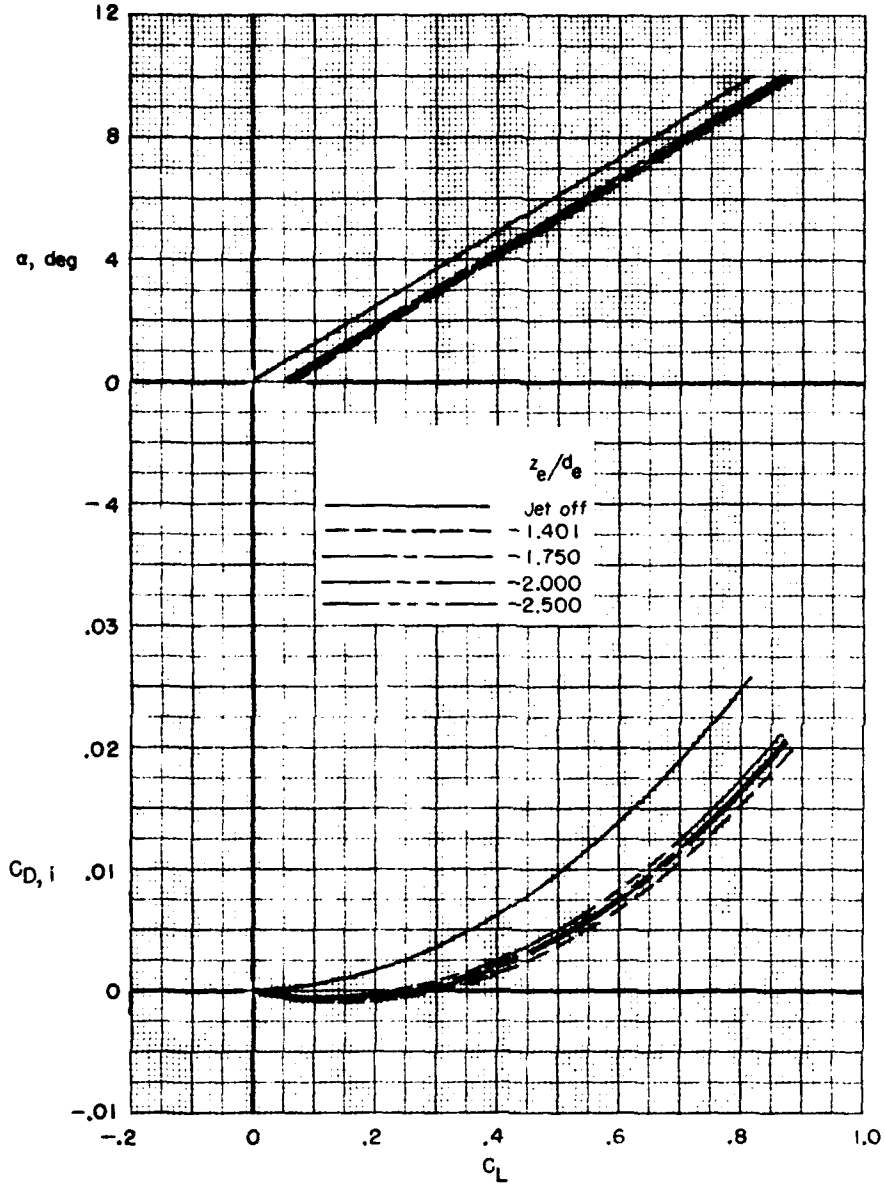

(a) Effect on C_L and $C_{D,i}$.

Figure 11.- Calculated effect of vertical location of two jets on aerodynamic characteristics of an AR = 8, λ = 1.0 straight wing. A_e/S_{ref} = 0.0125, V_e = 0.20, η_e = 0.25, $(x_e - x_{\ell e})/d_e$ = 0.0.

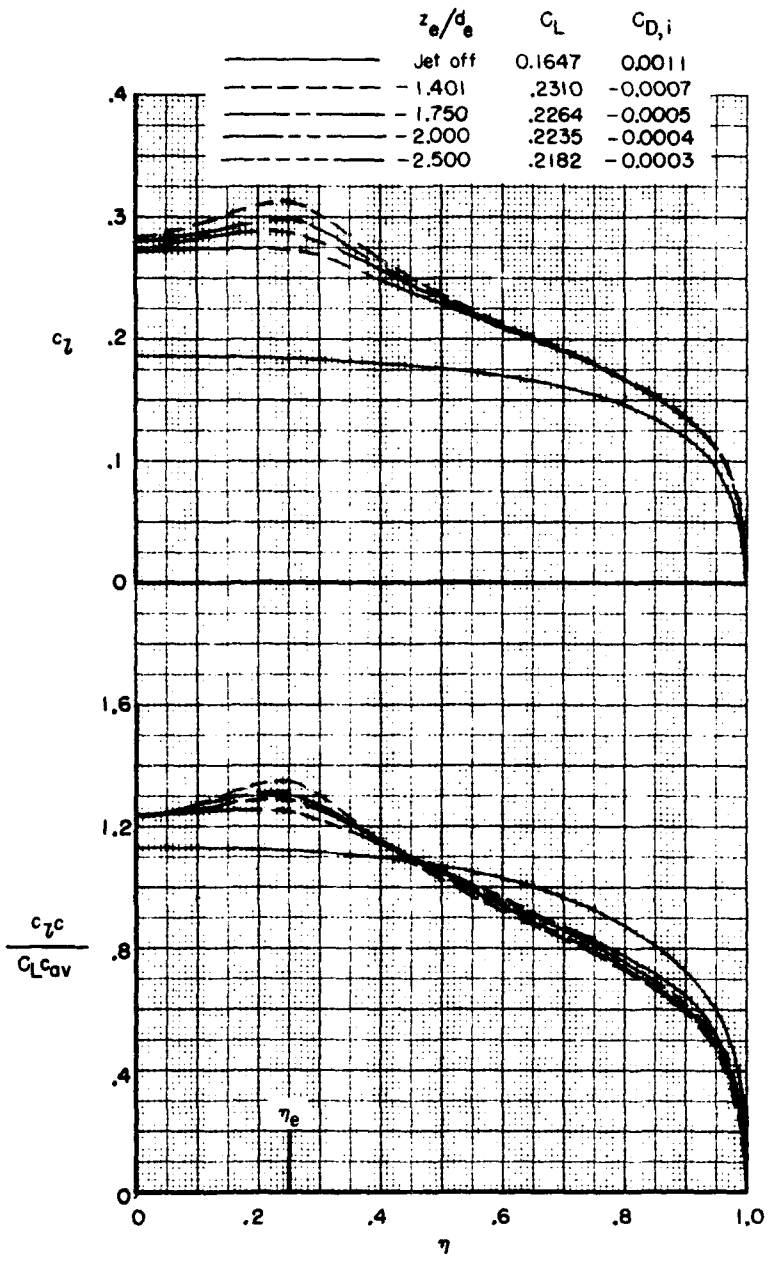

(b) Effect on span load distribution and section lift coefficient at $\alpha = 2^{\circ}$.

Figure 11.- Continued.

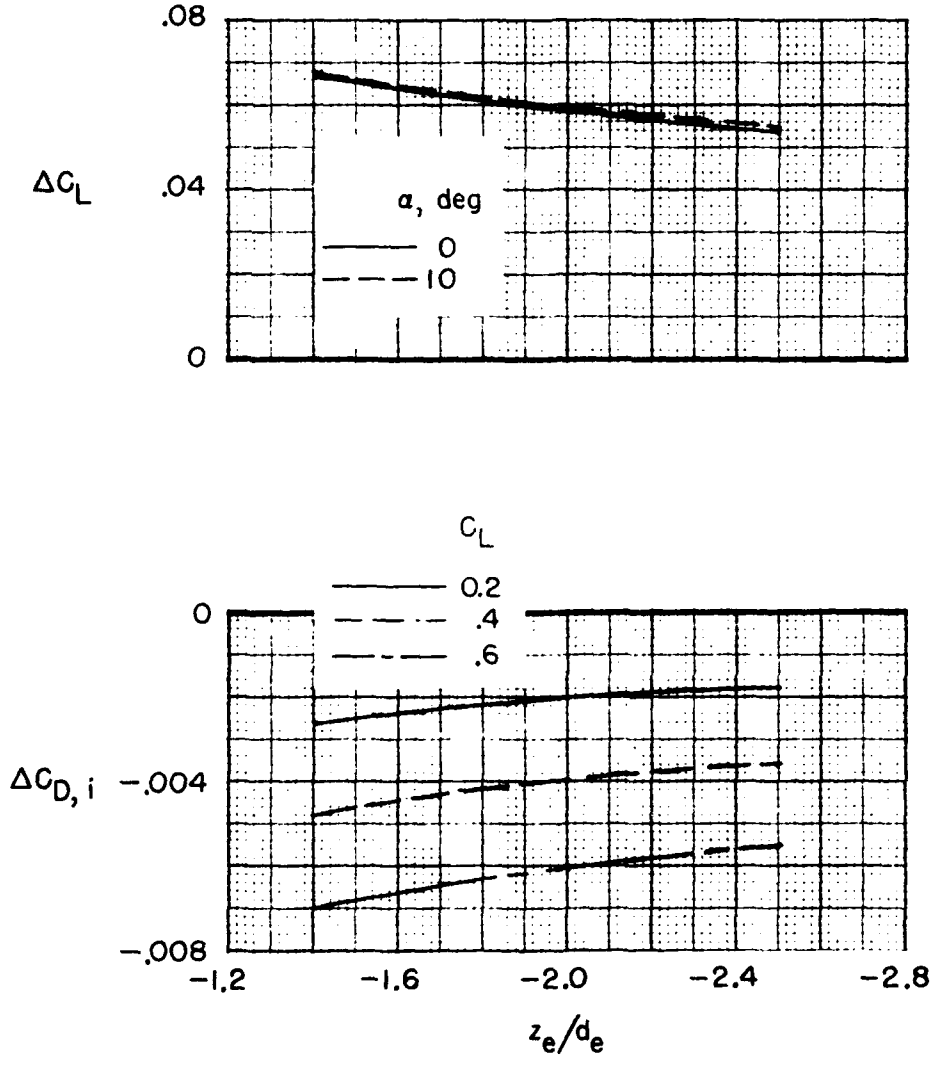

(c) Effect on ΔC_L and $\Delta C_{D,i}$.

Figure 11.- Concluded.

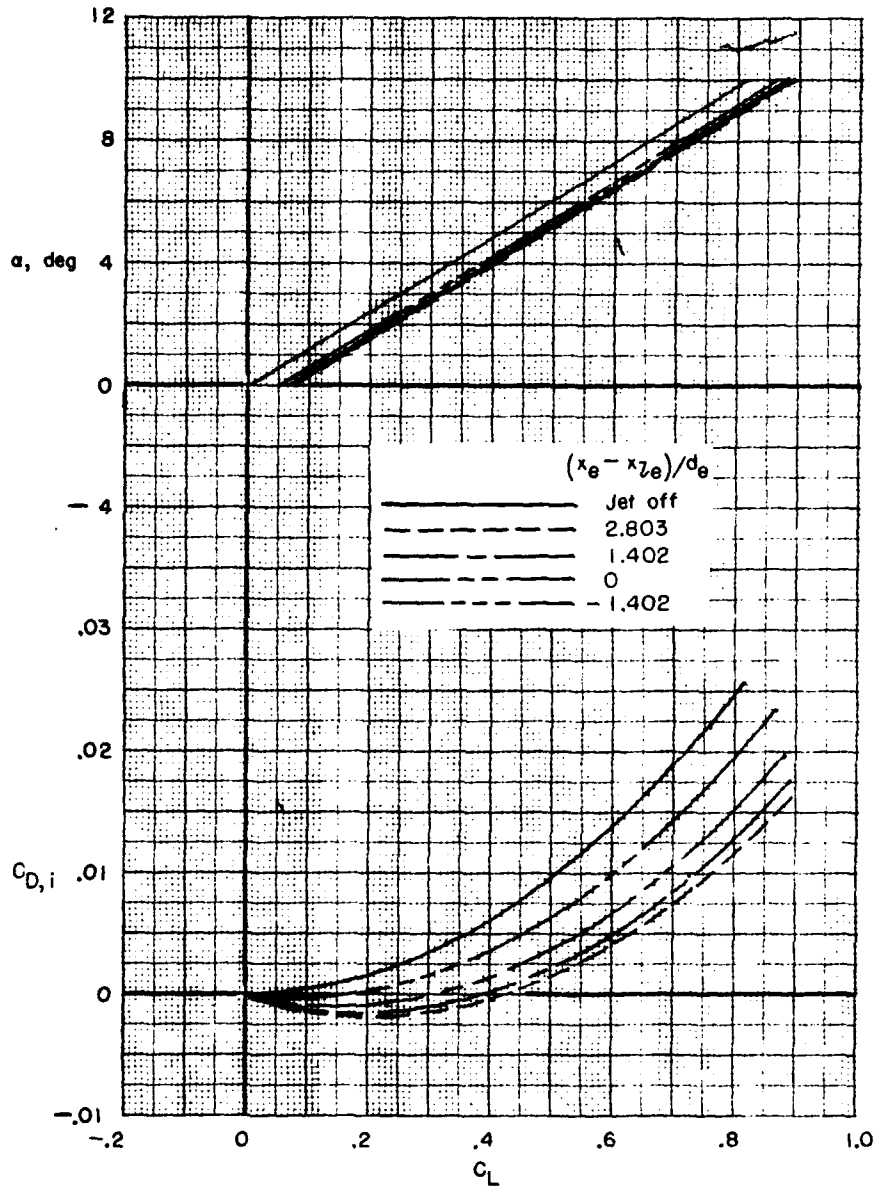

(a) Effect on C_L and $C_{D,i}$.

Figure 12.- Calculated effect of longitudinal location of two jets on aerodynamic characteristics of an AR = 8, λ = 1.0 straight wing. A_e/S_{ref} = 0.0125, V_e = 0.20, η_e = 0.25, z_e/d_e = -1.401.

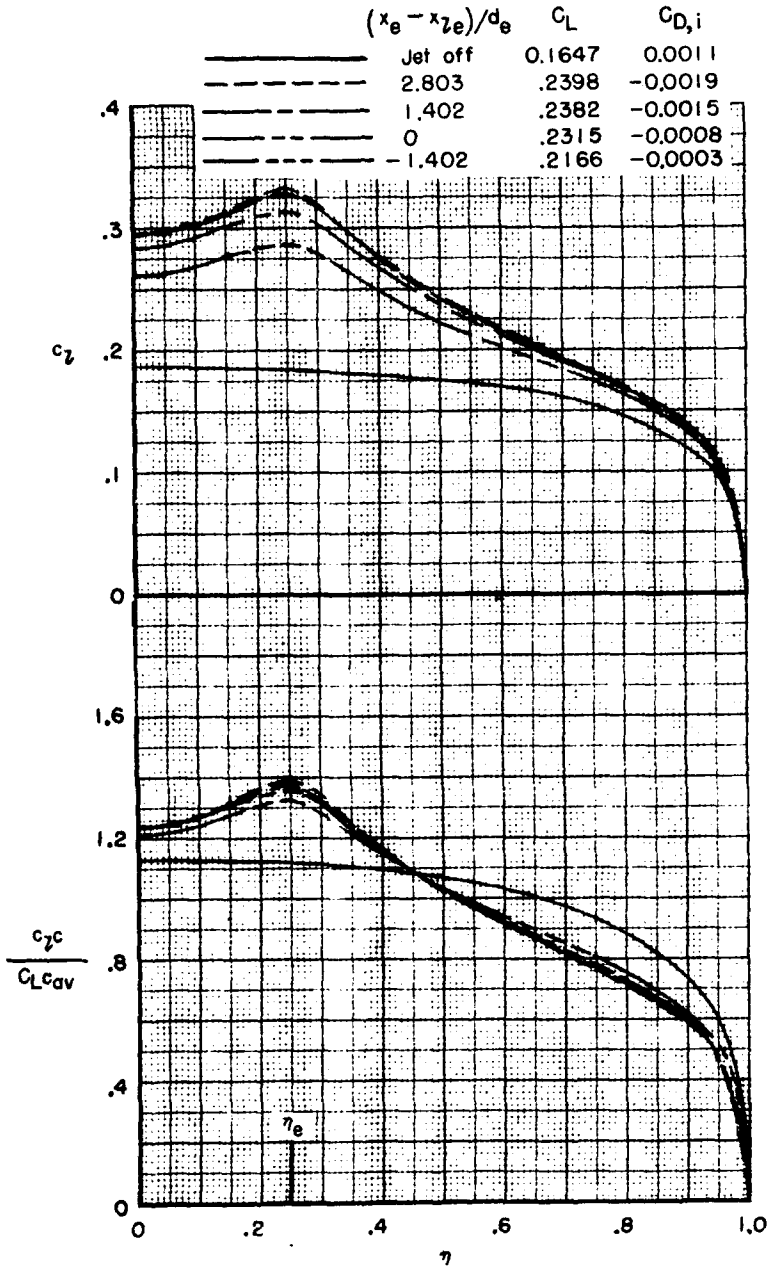

(b) Effect on span load distribution and section lift coefficient at $\alpha = 2^\circ$.

Figure 12.- Continued.

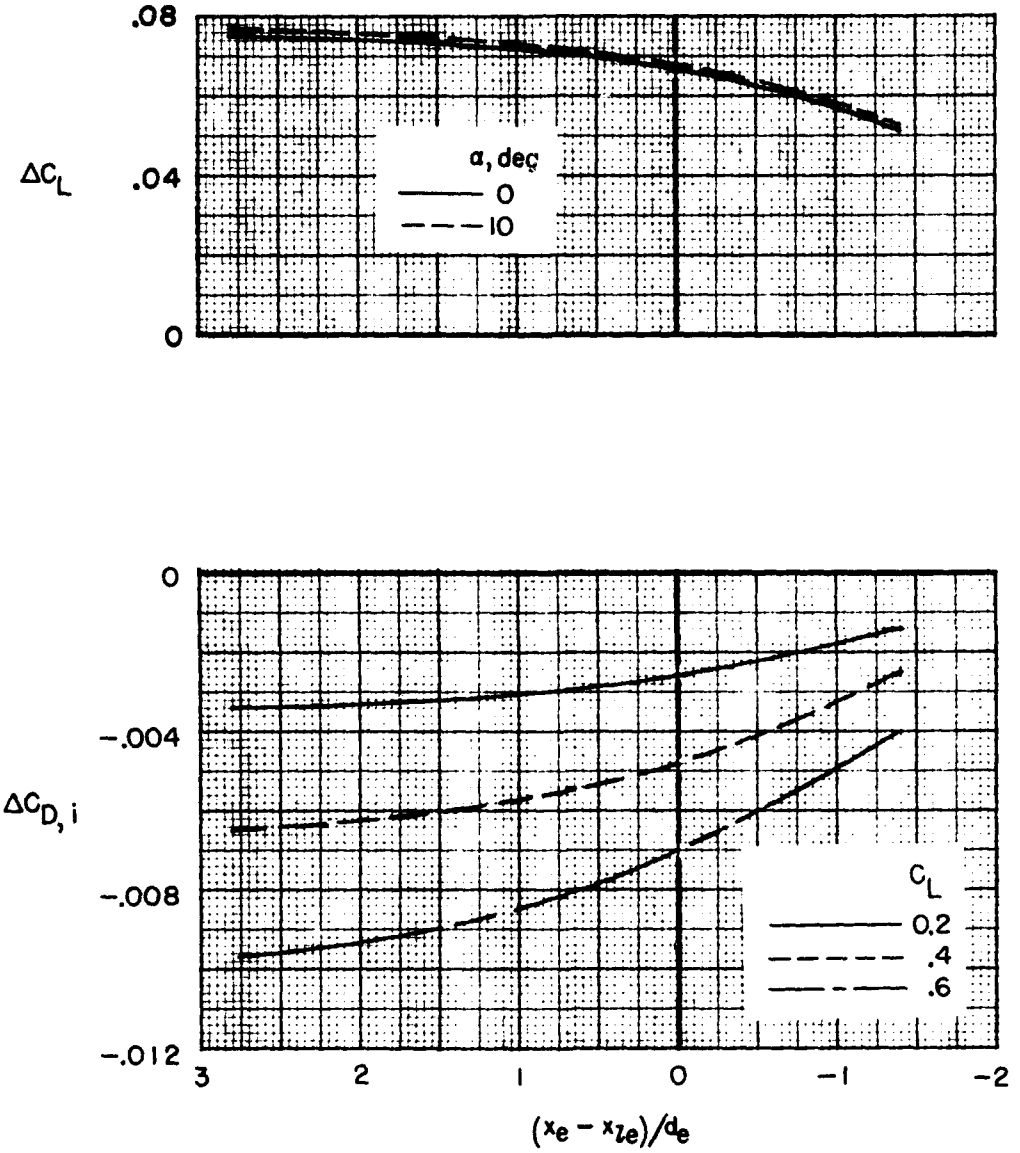

(c) Effect on ΔC_L and $\Delta C_{D,i}$.

Figure 12.- Concluded.

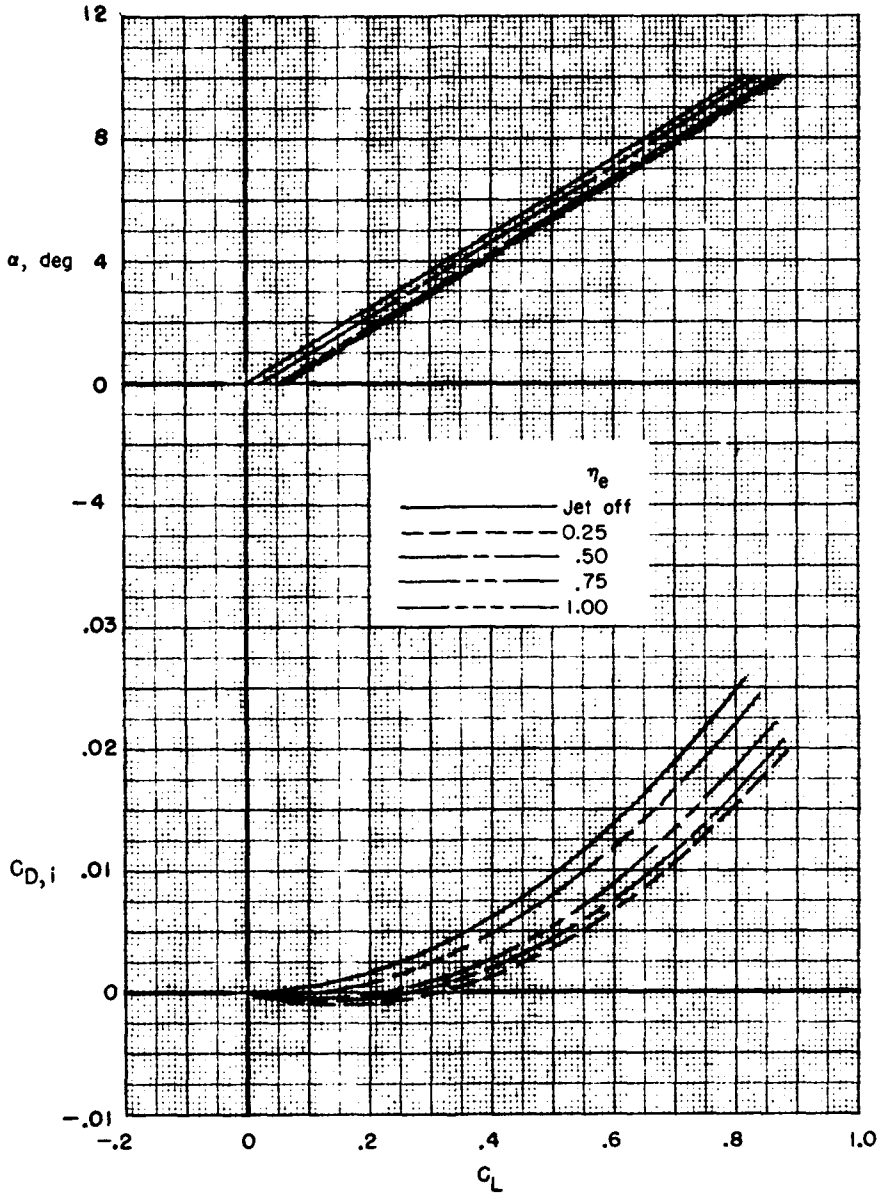

(a) Effect on C_L and $C_{D,i}$.

Figure 13.- Calculated effect of lateral location of two jets on aerodynamic characteristics of an AR = 8, λ = 1.0 straight wing. A_e/S_{ref} = 0.0125, V_e = 0.20, $(x_e - x_{le})/d_e$ = 0.0, z_e/d_e = -1.401.

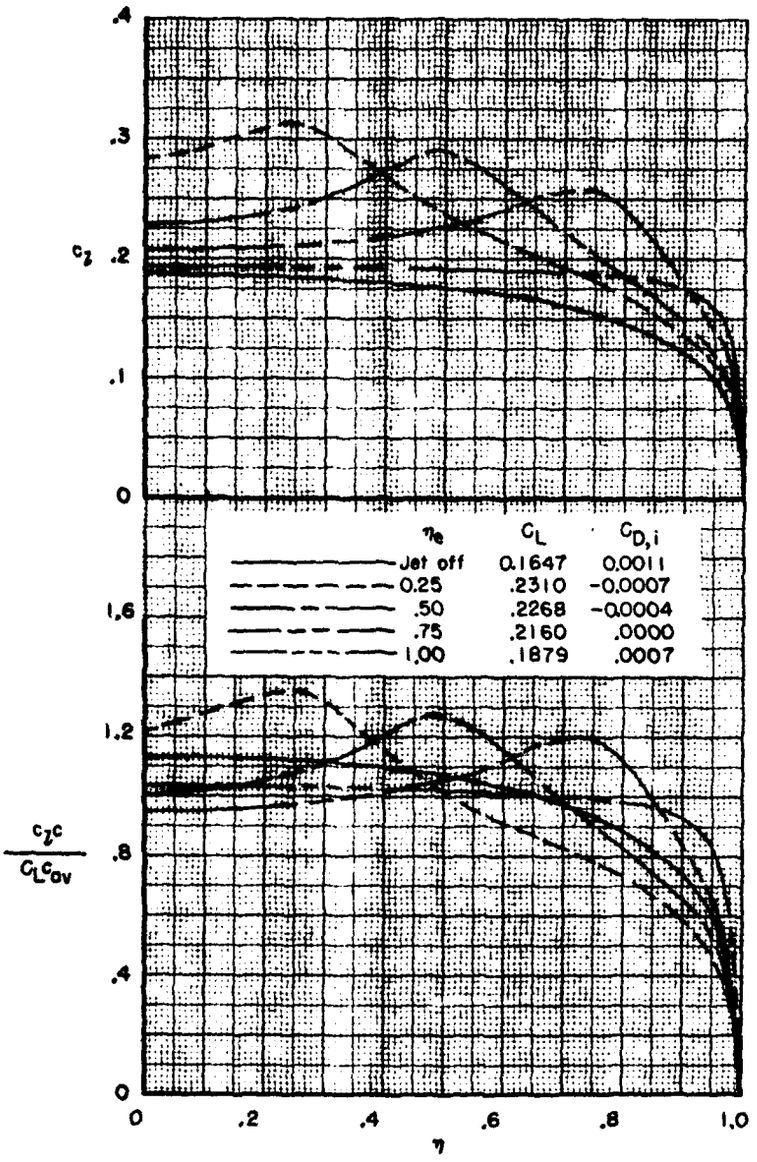

(b) Effect on span load distribution and section lift coefficient at $\alpha = 2^{\circ}$.

Figure 13.- Continued.

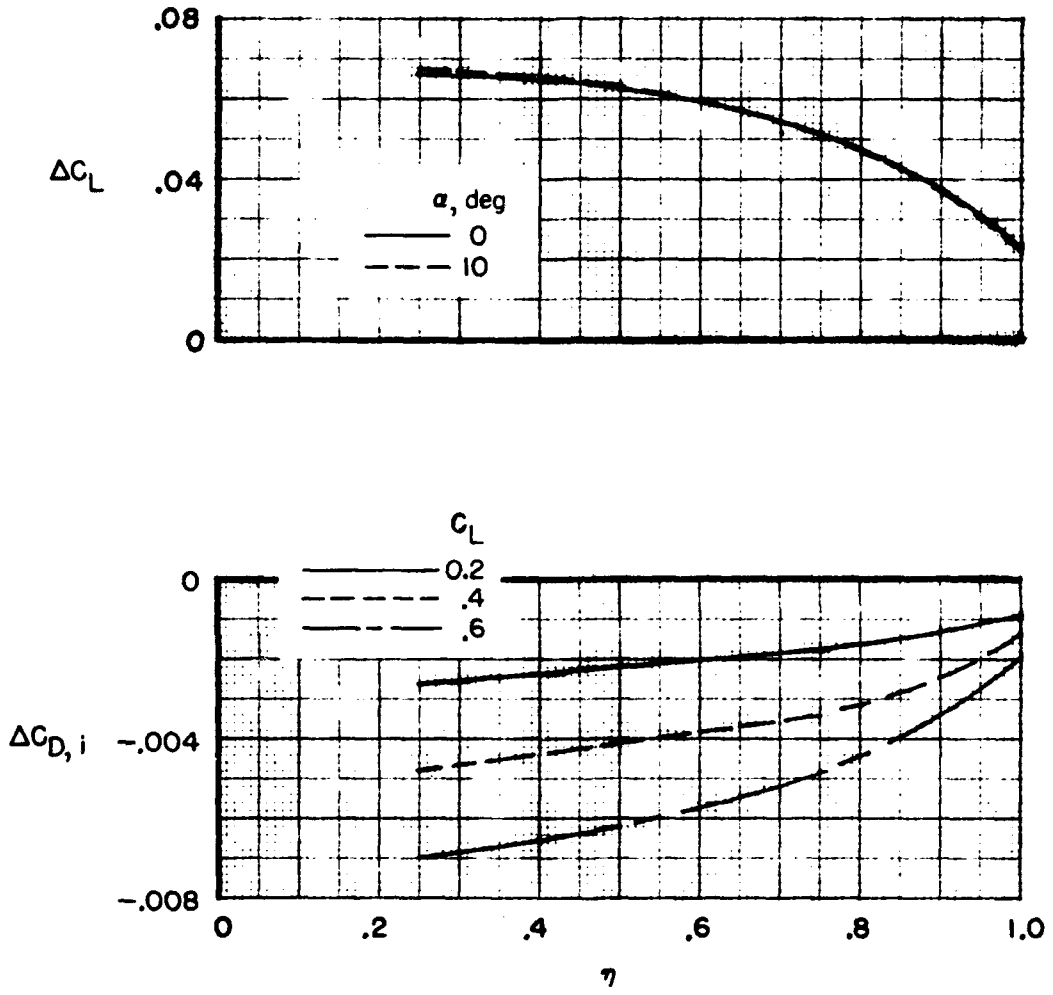

(c) Effect on ΔC_L and $\Delta C_{D,i}$.

Figure 13.- Concluded.

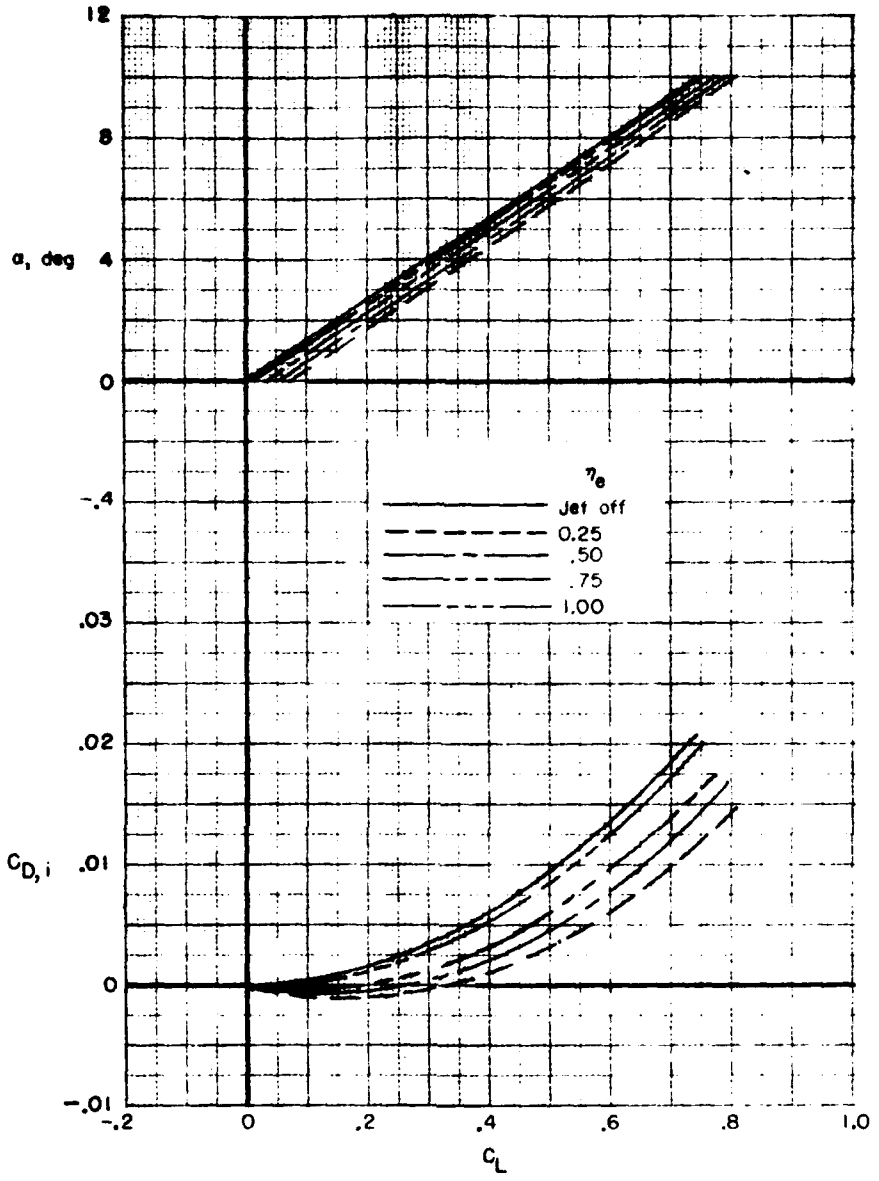

(a) Effect on C_L and $C_{D,i}$.

Figure 14.- Calculated effect of lateral location of two jets on aerodynamic characteristics of a wing with AR = 8, λ = 0.3 and $\Lambda_{c/4}$ = 30°. A_e/S_{ref} = 0.0125, V_e = 0.20, $(x_e - x_{le})/d_e$ = 0.0, and z_e/d_e = -1.401.

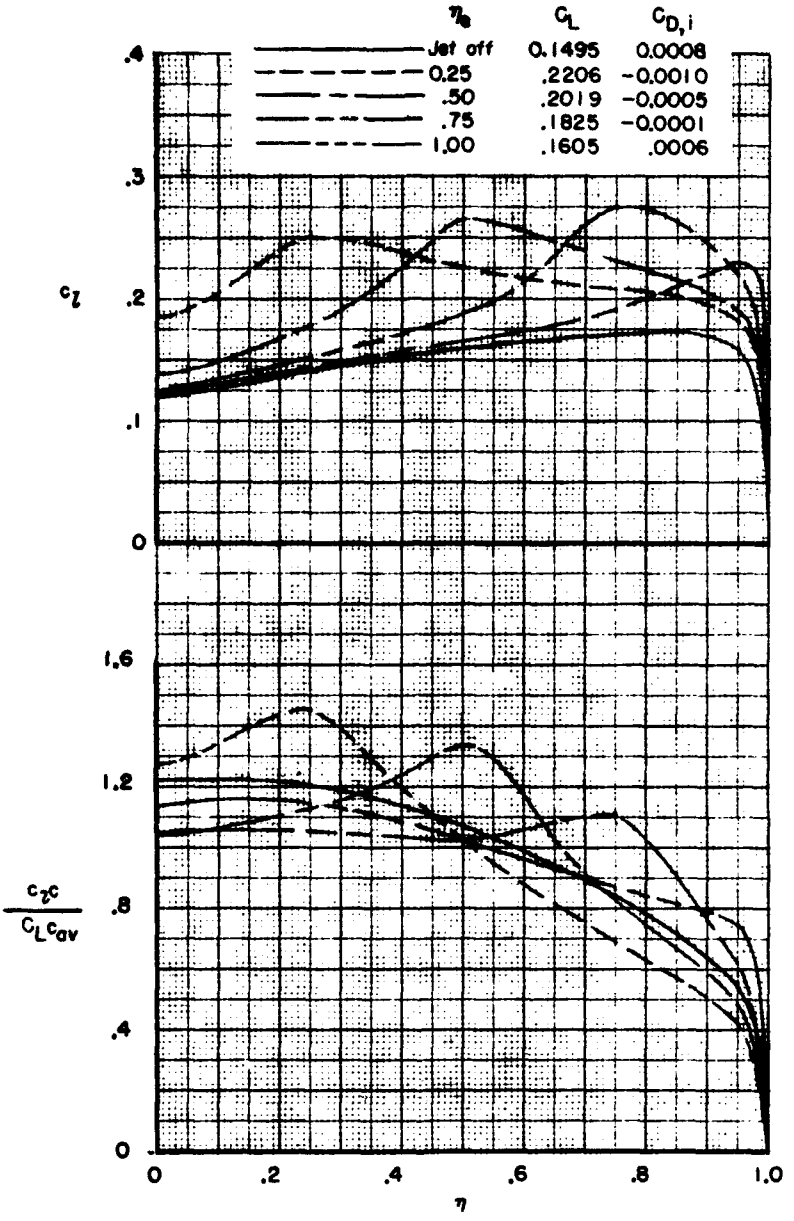

(b) Effect on span load distribution and section lift coefficient at $\alpha = 2^\circ$.

Figure 14.- Continued.

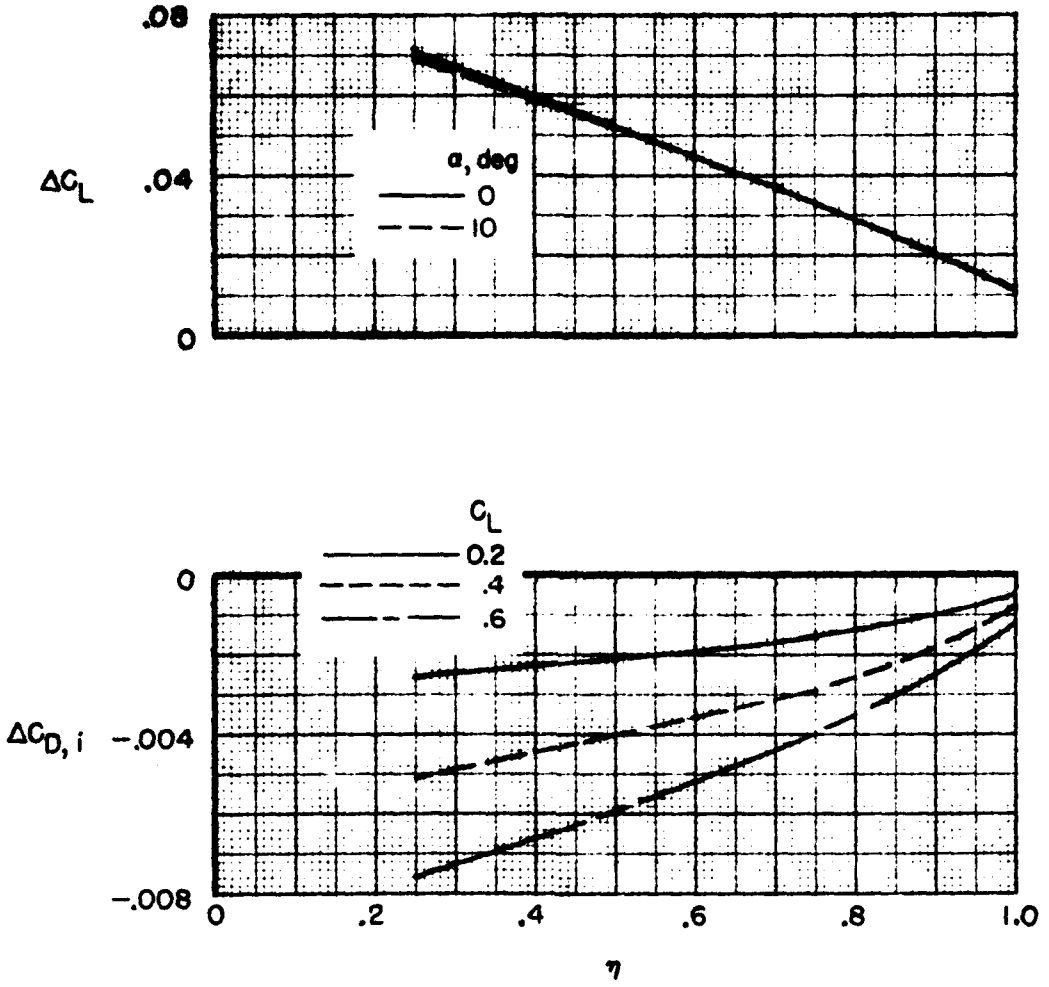

(c) Effect on ΔC_L and $\Delta C_{D,i}$.

Figure 14.- Concluded.